2011-01-01

Inhibition Of Calcium Oxalate Calculi By NDGA - A Spectroscopic Study

Preethi Dacha
University of Texas at El Paso, pdacha@miners.utep.edu

INHIBITION OF CALCIUM OXALATE CALCULI BY NDGA – A SPECTROSCOPIC STUDY

PREETHI DACHA

Department of Physics

APPROVED:

Felicia Manciu, Ph.D., Chair

Russell R. Chianelli, Ph.D.

Rosa Fitzgerald, Ph.D.

William Durrer, Ph.D.

Benjamin C. Flores, Ph.D.
Acting Dean of the Graduate School

INHIBITION OF CALCIUM OXALATE CALCULI BY NDGA – A SPECTROSCOPIC STUDY

by

PREETHI DACHA

THESIS

Presented to the Faculty of the Graduate School of

The University of Texas at El Paso

in Partial Fulfillment

of the Requirements

for the Degree of

MASTER OF SCIENCE

Department of Physics

THE UNIVERSITY OF TEXAS AT EL PASO

December 2011

ACKNOWLEDGEMENT

I would like to thank all people who have helped and inspired me during my study. First and foremost, I offer my sincere gratitude to my advisor Dr. Felicia Mancui, who has supported me throughout my thesis writing with lots of patience and knowledge. My special thanks to my advisor for giving me an opportunity to work with her. She shared her knowledge on experimental physics to be done. I really appreciate all her contributions of time, knowledge, and ideas. She was always kind towards me. During tough times in my Master's, she helped me a lot. She has given a lot of guidance from early stage of my research as well as provided me extraordinary experiences throughout the work. All her encouragement and efforts made me to accomplish my targets, without her presence my thesis wouldn't have been completed or written. I feel very lucky to have a very intelligent and friendly advisor. Dr. Manciu has been a true and caring advisor for me. I am very thankful for the excellent example she has provided as a successful women physicist and professor. I am extraordinarily fortunate to have Dr. Manciu as my advisor.

I also thank my graduate committee members Dr.Russell R. Chianelli, Dr. Rosa Fitzgerald, and Dr. William Durrer for agreeing in the committee as well as their support and guidance. I would like to thank R. Pal who is a Ph.D. student from chemistry department. He helped me in making the samples with a lot of patience. I would also like to thank The Department of Physics for financial assistance in my Master's degree. My deepest gratitude goes to my family for their love and supporting me to pursue the degree.

Finally, I would like to thank everyone who has supported for the successful completion of my thesis. Last but not least, thanks to God for giving me blissful life.

ABSTRACT

Formation of calculi in urinary tract leads to kidney stones. This process is known as Urolithiasis. Some of the causes of urolithiasis are metabolic disorders, genetic factors, and anatomic abnormalities in the urinary system. Nowadays, urolithiasis is very common disease in population of all over the world. The present study strives to understand calcium oxalate calculi formation as well as its inhibition by using Nordihydroguaiaretic acid (NDGA), which is a chemical extract of the Larrea Tridentata bush, a plant that is traditionally employed in the El paso region as a natural treatment for kidney stones and bladder diseases. Thus, in this current study, the crystals were synthesized without and with NDGA. This research is a continuation of previous efforts, which have demonstrated that the use of infusion from Larrea Tridentata decreases the sizes of calcium oxalate crystals and also changes their structure from a monohydrate for pure crystals to a dihydrate for crystals grown with different amounts of inhibitor. However, in the current study, both Raman and infrared absorption spectroscopic techniques, which are the methods of analysis employed in this work, reveal that NDGA is not responsible for the change in the morphology of calcium oxalate crystals and do not contribute significantly to the inhibition process. The presence of NDGA slightly affects the structure of the crystals by modifying the strength and length of the C-C bonds as seen in the Raman data. Also, the current infrared absorption results demonstrate the presence of NDGA in the samples through a strong absorption line that corresponds to the double bond between carbon atoms of the ester group of NDGA.

TABLE OF CONTENT

LIST OF FIGURES

Chapter 1: INTRODUCTION

1.1 INTRODUCTORY REMARKS

Urolithiasis refers to stones originating from the urinary tract. Urolithiasis, kidney stones, and renal calculi are terms which refer to the accumulation of hard, solid, and nonmetallic minerals in the urinary tract.[1] Nephrolithiasis and Ureterolithiasis refer to the accumulation of mineral deposits within the kidney and ureter, respectively. There are several conditions which contribute to kidney stone formation: a high concentration of stone forming mineral salts such as calcium oxalate and calcium phosphate in the urine; an uneven balance of acid in the urine; crystal growth mechanisms which prevent substances such as phosphates, citrates, and magnesium from remaining in solution in the urine.

There are four types of stones that form in the kidneys:

- Calcium stones: having too much calcium, oxalate or too little citrate in the urine causes calcium stones.
- Struvite stones: chemical alteration of urine leads to struvite stones which may lead to kidney infection.
- Uric acid stones: an excessive production of uric acid causes these stones.
- Cystine stones: these stones are due to a genetic disorder involving a gene coding for a cystine residue which results in an excess of cystine in the urine.

When the body's pH balance becomes too acidic or too basic, this causes accumulation of minerals that form kidney stones. Researchers suspect that high protein diets cause kidney

stones. When the digestive system digests protein, it breaks down into acids. The body balances the acidity with the available alkaline base: calcium (from bones). This results in deposition of calcium in the kidneys. The accumulation of calcium can form kidney stones.

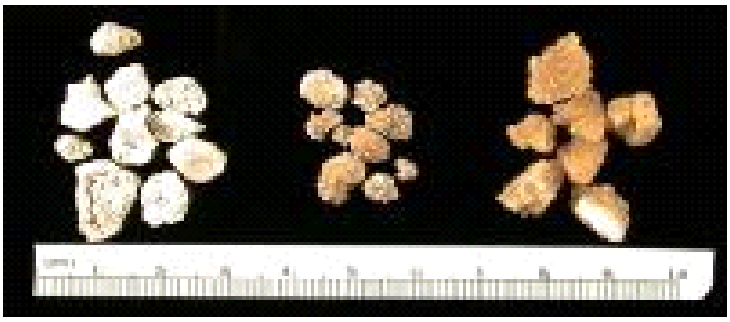

Figure 1.1: Stone groups containing different calcium, phosphate, and oxalate concentrations.[1]

Kidney stones are less common in children than in adults. Materials that create stones in children include calcium with phosphate or oxalate, purine derivatives, magnesium ammonium phosphate, cysteine, combinations of the preceding items, and drugs or their metabolites. The probability of developing kidney stones or other related problems after the first kidney stone depends on the child's age at the time of the first stone and the reason for the stone development. Studies show such chances to be between 30 and 65 percent.[2] Domesticated animals suffer from kidney and bladder stones similar to those found in humans.

An initial kidney stone symptom is extreme pain, which happens due to stone movement in the urinary tract that blocks the flow of urine. This severe pain tends to occur in the side and in the back below the ribs, and can spread to the lower abdomen and groin. Additional symptoms include nausea and vomiting, fever and chills if an infection is present, pain while urinating, and hemeturia (blood in the urine). One or more kidney stones can form in the

kidneys and result in renal colic. When a large kidney stone moves out of the kidney and into the ureter it causes the symptoms of renal colic. Renal colic can continue for hours to days.

Calcium oxalate monohydrate (COM), also known as the mineral whewellite with the formula $CaC_2O_4H_2O$, is the dominant crystal in the majority of kidney stones. This crystal is found in plants (cacti), coal, hydrothermal deposits, and sedimentary nodules. In several cases it occurs in micro crystal form instead of complex aggregates similar to kidney stones.

1.2 UROLITHIASIS EPIDEMIOLOGY

The recent studies of National Health and Nutrition Examination Survey (NHANES)II (1976 to 1980) and NHANES III (1988 to 1994) suggest that kidney stones, as a disease, is becoming more common. In the US, urolithiasis occurs more commonly in the southeast and Caucasian children are the most affected. Between two particular time periods, the presence of the disease in adults increased from 3.8% to 5.2%; it increased in all age groups and in both sexes, and in both African Americans and Caucasians in all age groups.[3] Urolithiasis epidemiology varies according to geographical area and historical period. Socio-economic affect lithiasis in terms of both the anatomical site and the physical/chemical composition of the calculi. In economically developed countries the rate occurrence of reno-ureteral calculosis varies between 4 and 20% and the annual incidence of hospitalization for calculosis ranges from 0.03 to 0.1%.[4] The age-adjusted prevalence was highest in the South (6.6%) and lowest in the West (3.3%). Factors that influence incidence rates are sex, age, race, and geographic region. Population-based estimates have ranged from 1 to 3 per 1,000 per year for men and 0.6 to 1.0 per 1,000 per year for women.[3] On the other side of the globe vesical calculusis is common in huge areas of Turkey, Iran, India, China, Indochina and Indonesia due to malnutrition early in life. The presence of kidney stones is due to environmental factors such as dietary intake and

lifestyle. In fact, genetic predisposition also plays a major role in the occurrence of calcium oxalate stones.

1.3 UROLITHIASIS TREATMENT

Generous fluid intake gives better results in urolithiasis treatment. Milk contains significant calcium and vitamin D. Orange juice may be supplemented with calcium. Tea contains oxalate and often sucrose. Many drinks (eg, sports drinks) contain sodium chloride and sucrose. While any fluid can be taken, water is the ideal fluid for passing out small stones in the ureter. An inadequate amount of fluid intake leads to urine concentration which in turn leads to risk of kidney stone formation. Larger stones may require treatment in order to achieve expulsion.

1.4 TYPES OF SURGICAL TREATMENTS

1. Extracorporeal shock-wave lithotripsy (ESWL), entailing frequent treatments and the power of shock waves
2. Percutaneous nephrolithotomy (PNL) with or without lithotripsy with US probes, electro-hydraulic, laser, or hydropneumatic probes
3. Retrograde removal of ureteral and renal stones (retrograde intrarenal surgery [RIRS])
4. Anesthesia (sedation, general anesthesia)
5. Open surgery
6. Laparoscopic surgery
7. Chemolytic percutaneous irrigation
8. Oral chemolysis
9. Treatment of staghorn stones

10. Management of complications of stone removal methods.[5]

1.5 MODERN MEDICINE

Urolithiasis treatment requires special equipment to treat patients. This treatment requires blood chemistry analysis and tests for inflammation, microbial infection, and blood in the urine. One of the main methods of examining the kidneys is the Ultrasonic procedure. This method identifies the stones and their movement, but ureteral stones are not visible in ultrasonography due to their lying deep in the retroperitoneal space. Excretory urography is a method which uses X-rays to snapshot the urinary system in order to determine the size and shape of stones. However, a few typical types of stones are not visible in photographs with this method. The Radioisotope procedure uses a special device for scanning the kidneys.[6] It is a modern and very informative means of investigation on enabling precise identification of renal dysfunction. Of course, these techniques require highly sophisticated instruments, which generally unavailable to many people. Traditional medicine can thus still play its role as a more convenient and widely accessible treatment.

1.6 TRADITIONAL MEDICINE

Traditional medicine or indigenous medicine encompasses medical knowledge acquired through the experience of many generations, even before the era of modern medicine. In Ancient times, the traditional medicine approach was the only way to treat diseases. Accumulated knowledge and practice is used in diagnosis and prevention and relies exclusively on practical experience; its observations are handed down from generation to generation. Well noted traditional medicines include herbal, Ayurveda, Siddha medicine, Unani, ancient Iranian medicine, Islamic medicine, traditional Chinese medicine, traditional Korean medicine,

acupuncture, traditional African medicine, and other medical knowledge and practices all over the globe. According to the World Health Organisation (WHO), traditional medicine is defined as "*the health practices, approaches, knowledge and beliefs incorporating plant, animal, and mineral-based medicines, spiritual therapies, manual techniques and exercises, applied singularly or in combination to treat, diagnose and prevent illnesses or maintain well-being*". It may also include formalized aspects of folk medicine, *i.e.* longstanding remedies passed on and practiced by lay people. Most of the people in Asia and Africa depend on traditional medicine for their primary health care needs. Even though people seek modern medicine, traditional medicine functions as complementary and alternative medicine.[7] The WHO also notes that "inappropriate use of traditional medicines or practices can have negative or dangerous effects" and that "further research is needed to ascertain the efficacy and safety" of several of the practices and medicinal plants used by traditional medicine systems. Ethnomedicine, ethnobotony, and medical anthropology are core disciplines.

Worldwide, 80% of the people rely on traditional medicine. The World Health Organization estimated that in Germany, 600-700 herbs are available and are approved by 70% of German physicians. For the past 20 years in the United States, popular interest has turned to natural or organic remedies, which has led to a drastic increase in traditional medicine use.

1.7 HERBAL MEDICINE

Herbal medicine is also known as botanical medicine or phytomedicine, using herbs seeds, berries, roots, leaves, bark, or flowers for medical purposes. It has a long history and tradition. Nowadays, it's becoming more widely accepted as improvements in analysis and quality control with advances in clinical research show the importance of herbal medicine. Ancient Chinese, Egyptian, and various other indigenous cultures used herbal medicine. All

parts of the world tended to use similar kinds of plants for the same purposes. In the 19th century, when chemical analysis became available, all over the world scientists began to extract the active ingredients from plants.

In the treatment of kidney stones, herbal medicine is playing a more prominent role than any other treatment. Herbal plants are used to breakup kidney stones and also to prevent new formation. They also help to relieve the irritated walls of the urinary tract. Hydrangea, Chanca piedra, Chaparral, Scoparia dulcis, Punarnava, Varuna, Tribulus, Shigru, Apamarg, and Horsetail are the herbal plants which are used for the best herbal remedies for kidney stones. Bearberry (Arctostaphylos uva-ursi), Cleavers (Galium aparine), Corn silk (Zea mays), Crampbark (Viburnum opulus), Kava kava (Piper methysticum) are herbs which are used to ease discomfort with stone passage. Herbal medicine doesn't have side effects if it is used in proper dosage. Along with the herbal remedies, an appropriate and balanced diet is essential to avoid kidney stones. This medicine approach is effective in treating kidney stones. Usage of herbal medicine has increased in various countries.

Across the world, predominantly India, China and various Arab countries are using herbal medicine. Chinese traditional medicine practices such as Liu Wei Di Huang and Shi Lin Tong are used to strengthen the kidneys as well as to dissolve the stones. Li Dan Pian herbal medicine is a treatment for gallstones. In India, Calcury is a special herbal mineral which prevents urinary tract infection and stone formation.[8] It helps to keep the urinary tract healthy and to maintain normal urine composition and mucosal integrity. It normalizes acidic urine and reduces pain. Moreover, it is anti-inflammatory, pain relieving, antibacterial and balances urine pH to avoid stone formation in the urinary tract. Carry mi seed, which grows in tropical parts of the world from the Amazon and Caribbean to India and China, has a long history in herbal

medicine.[9] Modern research studies have confirmed positive effects in using this herbal medicine for liver and urinary disorders. The herb is also reputed to be an effective treatment for kidney and gallbladder stones and other viral infections. In South and Central America, Carry mi herb is known as 'chanca piedra', due to its good reputation in treating such diseases.

1.8 COMPARISON WITH OTHER TREATMENTS

Modern medicine is dominant in developed countries; it has drawbacks such as high cost and side effects which tend to lead people to adopt herbal medicine. According to United States statistics, a large number of people die due to the incautious consumption of various medications. Most synthetic medicines are expensive; millions of people can't afford them. Shockwave lithotripsy is the modern treatment for kidney stones; this treatment uses laser technology, which has adverse effects. A laser beam breaks the kidney stones into small sizes and with excess intake of water helps to get rid of stones. This process can have various side effects; for example, higher risk for diabetes was related to the high intensity of the laser; risk of developing hypertension was highest when both kidneys were treated; this therapy can damage the pancreas and could alter the secretion of hormones originating in the kidneys, such as rennin, which influences blood pressure.

Percutaneous Nephrolithotomy is the type of surgery used to remove kidney stones. During this procedure, patients are given a anesthetic that has risks of long term consequences, which are mental confusion, stroke, lung infections, heart attack and sometimes leads to death. After the treatment patients experience pain and swelling at the incision site. In open surgery, doctors use a large incision in the patient's side so that they can reach the kidney and remove the stone. Due to the large incision, one can see severe side effects which include sharp, shooting

pain, nausea, vomiting, and fever or swelling around the incision area. Recovery from the symptoms takes several weeks.

Parathyroid surgery is one of the treatments for kidney stones. In some cases, malfunctioning parathyroid glands can cause kidney stones. Parathyroid glands may develop small cysts that cause the glands to become overactive and which raise the calcium level in the body and lead to kidney stones. For this particular problem, surgery is needed to remove the cysts. This surgery can include side effects such as injury of the laryngeal nerve, which controls the vocal cords, and sudden removal of the parathyroid gland can result in a hormonal imbalance called hypoparathyroidism.[10] Initially ureteroscopy is considered safe and effective. It has limitations due to regional restrictions and stone size, and is more invasive and has a higher risk of damage. Side effects of ureteroscopy are frequent urination, blood in the urine, stent discomfort and pain in the region of the kidneys, bladder and urethra. In lieu of modern surgery treatments, herbal medicine is considered the best way to treat and avoid kidney stones. Herbal medicine doesn't show any side effects if it is taken in proper dosage and is also inexpensive medicine.

1.9 LITERATURE REVIEW

Kidney stone treatment requires knowledge of the chemical composition and structure of stones. Both physical and chemical techniques are used for urinary stone analysis. Advanced techniques such as CT scanning are generally necessary for analysis before the choice of treatment is finalized. Urinary stone analysis depends mostly on chemical rather than physical analytic techniques. Chemical analytic techniques detect individual stone composition. In the nineties, there was an apparent increase in the use of physical analytic techniques such as infrared spectroscopy and x-ray diffraction photography. [11] On the other hand, the new

technique fibreoptic infrared spectroscopy represents a new analytic trend in urolithiasis. This technique is designed to provide an advanced analysis, qualitatively and quantitatively of the various urinary salts.

The research group of Daudon *et al.* analyzed a series of 10,617 calculi by stereomicroscopy and infrared spectroscopy. They were first in finding that the frequency of pure calculi was the lowest. Calcium oxalate (86.48%) was the component most frequently present, next follow calcium phosphate (79.75%) and purines (18.64%).[12] Composition varies depending on sex; for instance, Calcium oxalate dihydrate (COD) was more common in men than in women. On the other hand, calcium phosphate was more frequent in women. In French patients, COD calculi were most common in stone formation. Compositions also depend on age, socioeconomic conditions, geographical area, and diet. Avoub Kamoun *et al.* group analyzed 120 Tunisian patients in an age group from 5 months to 15 years from. They found in 91 cases (76%) that the stone was located in the upper urinary tract. Urinary stone analysis requires both morphological examination and an infrared analysis of the nucleus and the inner and peripheral layers. The bladder stone nucleus is composed of ammonium urate (45%), struvite (28%), cystine (10%), and carbapatite (13%).[12] Depending on stone composition, urinary tract infection sometimes accompanied nucleation. On the contrary, less than 25% of the cases were based on metabolic factors – genetic diseases such as hyperoxaluria, cystinuria, and hypercalcuria were responsible.

Yi-Chun Chiu *et al.* analyzed urolithiasis using Raman spectroscopy because it is a common disease with high recurrence rate (60% in five years), so proper diagnosis is necessary. Uretroscopy, lithotripsy, and extracorporal shock wave lithotripsy were helpful in the breakdown of large kidney stones into small fragments and these small powdered stones were collected in

the urine. Raman spectroscopy was used in the analysis of the tiny fragments of stones which were collected from patients' urine after the medical surgical treatment. From Raman, data was collected and five types of primary stones were found; they are calcium oxalate monohydrate (COM), dicalcium phosphate dihydrate (DCPD), calcium phosphate hydroxide (CPH), calcium oxalate dihydrate (COD), and uric acid. They used Raman and FTIR spectroscopy to analyze stones and examined seventeen different patients' urine. They succeeded in measuring COM, DCPD, CPH, COD, and uric acid.[13] The FTIR spectroscopy database showed that 234 (37.4%) were pure, and the most common was calcium oxalate (33.9%), followed by calcium phosphate (2.7%), and uric acid (0.8%). Also, 391 (62.6%) were mixed stone, calcium oxalate (43.2%) was the most frequent component, followed by calcium phosphate (16.3%), cystine (1.3%), uric acid (1.1%), and struvite (0.6%). Uric acid was the major component found most frequently in men, whereas struvite was more frequent in women.[14] Uric acid was more common in lower urinary tract stones. In eastern China, calcium oxalate was most commonly found, though the most recurrent mixed stone was a calcium oxalate and calcium phosphate mixture. Geographic location, gender, and age have a major influence on stone composition.[15]

Apart from Raman and FTIR, a urolithiasis study was done using optical microscopy and scanning electron microscopy (SEM). In many clinical centers, stone analysis is incomplete. Stone composition identification is essential for deciding future prophylaxis. X-ray diffraction, Fourier transform infrared spectroscopy, and scanning electron microscopy (SEM) still remain distant dreams for routine work. An alternative procedure is optical microscopy. Optical microscopy gives a magnification of up to 40X and a clear picture of the stone surface. In order to analyze urinary stones, SEM and elemental distribution analysis have been performed.[16] A total of 250 urinary stones of different compositions was collected from stone clinic. Optical

photographs were taken at different angles with magnifications up to 4,000. Under optical microscopy, appearances of stones were standardized, namely, bosselations of pure whewellite, spiculations of weddellite, uric acid appearing as bright yellow colored, and phosphates of dirty white amorphous color.[16] SEM and EDAX give clearer pictures and confirm stone composition. The higher magnification of SEM and EDAX are useful to provide a reference basis for performing optical microscopy work. The advantage of the optical microscope is that it is easy to use and its images can be analyzed in natural color.

Recently, research has concentrated on growing calcium oxalate samples in the laboratory using a single diffusion gel method. These samples were analyzed under Raman and FTIR spectroscopy. The single diffusion gel technique was used to grow calcium oxalate monohydrate, which is known as a urinary stone. Valarmathi *et al.* observed these crystals under FTIR and from the spectra they found various vibrational modes and also particular functional groups. These investigations revealed the existence of oxalate functional groups and water molecules in COM. Various methods were introduced for the growth of calcium oxalate in silica and gelatin gels under different conditions. In silica gel, calcium oxalate grows in single individual crystals, twins, and rosettes, whereas bipyramidal calcium oxalate dihydrate crystals were similar to crystals present in urine. In gelatin gel, calcium oxalate monohydrate crystals grow into aggregates. The gelatin medium is growth supporting and the process is controlled by stereospecificity.[17] The COM forms in the shape of splices, twins, spherulites and dendrites. Petrova *et al.* found, using atomic force microscopy, the growth and dissolution of calcium oxalate monohydrate (COM) crystals up to 30 μm in length. The rate of COM dissolution increased in the presence of aluminum and iron ions as well as with the substitution of Aqua RX water.[18]

Limited medical studies have used modern spectroscopy on herbal medicine. Recent research has focused on the analysis of traditional medicine by spectroscopic techniques. Spectroscopy was applied to the analysis of inhibited calculi growth from laboratory synthesis of calcium oxalate crystals.

To treat kidney stones, nowadays, a large amount of research focuses on spectroscopic study with the infusion of herbal extract. Joshi *et al.* worked on herbal extracts of Tribulus terrestris and Bergenia ligulata. Initially, COM crystals were grown by a double diffusion gel growth technique using U-tubes. They were prepared in a hydrated sodium metasilicate solution and nutrients were supplied for the growth. Tribulus terrestris and Bergenia ligulata were generally used as herbal medicines for urinary calculi in India.[35] In order to verify the inhibition effects of this herbal plant, herbal extract was added to the supernatant solutions. The growth was measured with and without the herbal extracts.

Later, detailed scientific studies were done by F.S. Manciu's research group on calcium oxalate calculi inhibition by Larrea Tridentata herbal extract and on struvite calculi formation under the influence of the *Rotula Aquatica Lour* plant. Besides an obvious decrease in the crystal sizes and a visible color change for the crystals grown with the herbal extracts, these researchers demonstrate, by using infrared (IR) absorption and Raman spectroscopy, mechanisms that potentially contribute to the inhibition processes.

Chapter 2: EXPERIMENTAL DETAILS

2.1 INTRODUCTION TO SPECTROSCOPIC METHODS

Spectroscopy is the study of interaction between matter and radiated energy. It is used in the physical and analytical chemistry of materials, since, due to internal arrangements of atoms and molecules, every substance has a unique spectrum. Consequently, it is used to detect, identify, and quantify chemicals. It is also worth noting that to gain information on material chemical composition, concentration, morphology, and bonding states, modern analysis requires multiple investigation techniques such as Raman scattering and infrared absorption spectroscopies, scanning electron microscopy (SEM), and X-ray Diffraction. Since this work is based on the information that can be acquired from the first two techniques, we are going to concentrate on these methods.

In its interaction with matter, light, which is a form of electromagnetic radiation, can undergo three effects: it can be transmitted, absorbed or scattered. The Fourier transform infrared (FT-IR) technique is concerned with the first two, while Raman is concerned with the latter. FT-IR and confocal Raman spectroscopies are two powerful characterization methods which complement each other in providing information regarding the chemical nature and structural properties of the bonding between atoms. Underlying this complementarity are the differences in the mechanisms of photon energy transfer that are affected by the structure and the symmetry characteristics of the sample under study, as explained in detail below. Thus, by employing both spectroscopic techniques, the ability to look at all active vibrational and rotational levels of molecules for a complete characterization of the sample is available.

2.2 RAMAN SPECTROSCOPY

Raman scattering or the Raman effect is the inelastic scattering of a photon, which was discovered by Sir C V Raman. In this inelastic scattering, the frequency of monochromatic light changes with interaction with a sample in the sense that the reemitted photon frequency is shifted up or down as compared with the incident photon frequency.[19,20] This shift in frequency gives information about vibrational, rotational, and other low frequency transitions in molecules.[19,20] Although, typically, Raman spectroscopy is mainly applied to multi-component analysis and, indirectly, to structure determination, it can also be used for quantitative and qualitative studies, since, not only frequency shifting information, but also the intensity, at specific wavelengths, of light scattered inelastically from molecules can be measured. Nowadays, Raman spectroscopy plays a crucial role in the analysis of an enormous variety of samples such as polymers, thin films, semiconductors, pharmaceuticals, fullerenes, and other carbon nonmaterials.

The Raman effect can be described in two ways: by a classical physical approach or by a quantum explanation.

2.2.1 Classical approach

For vibration to be Raman active, it must occur with a change in the polarizability of the molecule. A detailed explanation of this process is as follows: when the electric field component of the electromagnetic radiation (light) is interacting with a molecule, it will induce a dipole moment. This induced dipole moment, which is a vector, and the electric field are related by a property called polarizability, as described by the relation below:[21]

$$p = \alpha(Q) \cdot E = \alpha(Q) \cdot E_0 \cos(\omega_L t) \qquad (1)$$

where p is the dipole moment, α is the polarizability, and E is the electric field which has a maximum amplitude of E_0 and depends on the light's angular frequency ω_L.

Also, polarizability, which is a tensor depending on the vibrational coordinate Q, is a measure of the deformability of the electron cloud of the molecule by the electric field. The vibrational coordinate, Q, depends on the molecular vibrational angular frequency, ω_M, as follows:

$$Q = Q_0 \cdot \cos(\omega_M t) \tag{2}$$

Thus, the change in polarizability gives rise to amplitude modulation, at certain frequencies, of the induced dipole moment oscillation, which gives rise to the Raman frequency components.[21] This statement is easier understood if the Taylor series expansion of the polarizability:

$$\alpha = \alpha_0 + \left[\frac{\partial \alpha}{\partial Q}\right] \cdot Q + ... \tag{3}$$

is substituted into the expression of the induced dipole moment (Eq. (1)) to obtain the first-order expression:

$$\begin{aligned} p &= \alpha_0 \cdot E_0 \cos(\omega_L t) + \left[\frac{\partial \alpha}{\partial Q}\right] \cdot Q_0 \cdot E_0 \cos(\omega_M t) \cdot \cos(\omega_L t) \\ p &= \alpha_0 \cdot E_0 \cos(\omega_L t) + \left[\frac{\partial \alpha}{\partial Q}\right] \cdot \frac{Q_0 \cdot E_0}{2} \{\cos[(\omega_L - \omega_M) t] + \cos[(\omega_L + \omega_M) t]\} \end{aligned} \tag{4}$$

The first term in this expression for the induced dipole moment (Eq. (4)) has the frequency of the scattered light the same as that of the incident light and this term describes what

is called Rayleigh scattering or elastic scattering. The other two terms are for scattered light at lower and higher frequencies, respectively, and their respective effects are called Stokes and anti-Stokes scattering.

2.2.2 Quantum approach

The quantum explanation for Raman scattering, which is presented in Fig. 1, is clearer and pictorial.[22] The incident light energy excites the molecule from its ground state to the virtual state. The electron in the virtual state does not stay and immediately goes to the final ground state.

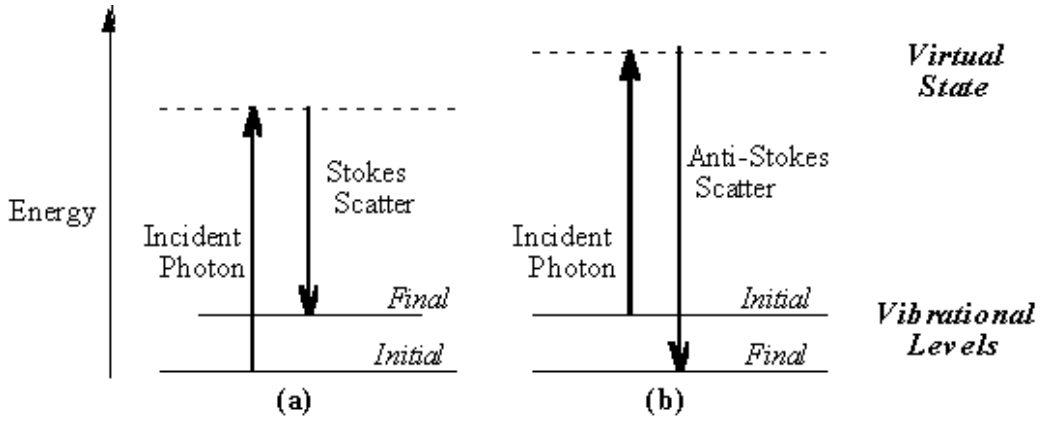

Figure 2.1: Energy level diagram in Raman scattering[22]

The Raman frequency shift is calculated using following equation:

$$\frac{\Delta\omega}{2\pi c} = \left(\frac{1}{\lambda_L} - \frac{1}{\lambda_S} \right) \qquad (5)$$

where c is the speed of light in a vacuum, $\Delta\omega$ is the Raman shift, λ_L is excitation wavelength, and λ_S is the Raman scattered wavelength. For the inelasting scattering, as mentioned above, there are two different processes occurring:

(1) When a photon from a source with angular frequency ω_L excites a molecule, the molecule absorbs a portion of the light energy and emits scattered light with the angular frequency $\omega_L - \omega_M$. This shift in frequency is known as a Stokes shift.

(2) When a photon with angular frequency ω_L is absorbed by an already excited molecule that also has the capacity to emit light containing more energy than it originally absorbed. The resulting scattered light's angular frequency is $\omega_L + \omega_M$. This shift in frequency is known as an anti-Stokes shift.

In spontaneous Raman, about 99.999% of the photons of the incident light undergo elastic Rayleigh scattering. This type of signal is not useful in molecular characterization. The remaining incident light, about 0.001%, produces inelastic scattering. Thus, spontaneous Raman scattering is very weak, and the main difficulty with Raman spectroscopy is the inalibity to distinguish the weak inelastic scattering from the intense Rayleigh scattered light. To obtain high quality Raman spectra, besides the use of high-resolution detectors, other instruments such as notch filters, tunable filters, laser stop apertures, and double and triple spectroscopic systems are employed to reduce the Rayleigh scattering.

Normally, Raman signals are quite weak and scientists are improving Raman techniques in order to enhance the intensity of the Raman signal.[19,20] Many types of advanced Raman spectroscopy techniques are now employe, including surface enhanced Raman, resonance Raman, tip enhanced Raman, polarized Raman, stimulated Raman, transmission Raman, spatially offset Raman, and hyper Raman.[19,20]

2.2.3 Raman experimental set-up

For the work presented here, Raman measurements were recorded with an *alpha 300 WITec* confocal Raman system using the 532 nm excitation of a Nd:YAG laser and a 20X objective. The system in the Optical Spectroscopy and Microscopy Laboratory is shown in Fig. 2, below.

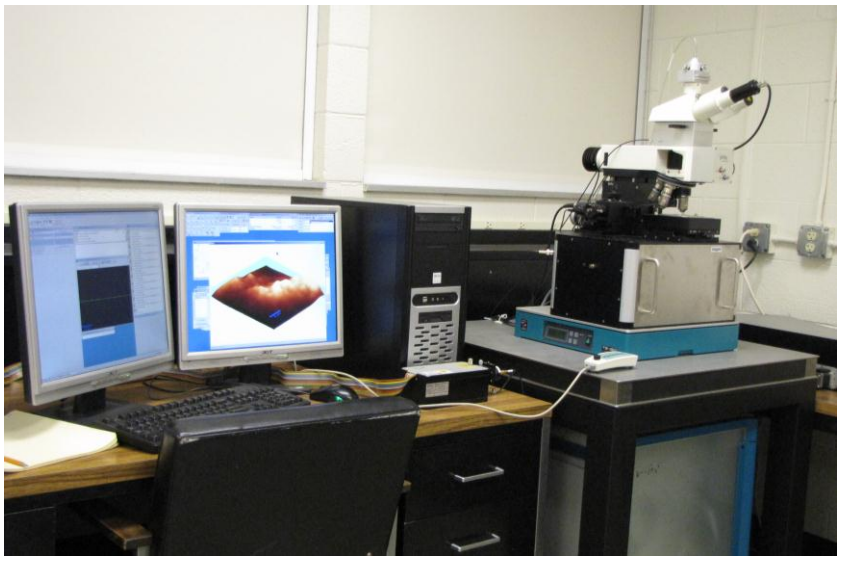

Figure2.2: *alpha 300 WITec* confocal Raman system.[34]

2.3 FOURIER TRANSFORM INFRARED SPECTROSCOPY

Fourier transform infrared spectroscopy (FT-IR) is a chemically specific analysis technique which can be used to identify chemical compounds, functional groups, and the molecular structure of organic and inorganic materials.[23] The Fourier transformation, which is a mathematical algorithm, originates from the requirement of converting the raw data into the actual spectrum. The Fourier transform approach implies that different frequencies are not directly separated out spatially, but instead a signal (an interference pattern) is generated vs. the

distance travelled by a moving mirror; this permits frequency separation by means of a Fourier transform computation.

FT-IR is an ideal spectroscopic characterization method as compared with other dispersive or filter methodologies for the following reasons: it is a non-dispersive and a non-destructive technique; it provides a precise measurement without the requirements of an external calibration; it has increased speed of data collection (a scan every second); it has increased sensitivity; and it is mechanically simple to operate.[24] With modern software algorithms, FT-IR spectroscopy is an excellent tool for quantitative analysis too.

In FT-IR spectroscopy, infrared radiation is passed through the sample; part of the radiation is absorbed by the sample and part is transmitted. The scattering component is usually neglected, since it is very small as compared to the absorbed or transmitted components. Thus, the spectrum obtained from FT-IR analysis represents the molecular absorption or transmission of the sample. No two different molecular structures produce the same infrared spectrum, similarly to a fingerprint. So, infrared spectroscopy is useful for several types of analysis, such as qualitative and quantitative. It has been used to determine unknown materials, their quality or consistency, and the number of components in a mixture.

A more elaborate description of the process is as follows: molecular bonds vibrate at several specific frequencies depending on the type of bond and the elements involved. These frequencies depend on the ground state and excited states. When the energy is absorbed by a molecule, the frequency of a molecular vibration can increase to excite a bond.

The difference in Energy States = Energy of Light Absorbed:

$$E_1 - E_0 = h\,c / \lambda \qquad (6)$$

where h is Planck's constant, c is the speed of light, and λ is the wavelength of the absorbed light.

Energetically, these transitions between molecular vibrational states generally absorb about 1-10 kilocalories/mole. This energy also corresponds to the infrared range in the electromagnetic spectrum; roughly between 13,000 and 10 cm^{-1}, in standard units of FT-IR spectroscopy, *e.g.* wavenumbers (cm^{-1}),or wavelengths from 0.78 to 1000 μm,.[25,26,27]

The Fourier transform spectrometer, which is the most important part of the system, is based on the Michelson interferometer with a movable mirror, which depends on the same principle as the Michelson Morley experiment and is schematically presented in Fig. 3.

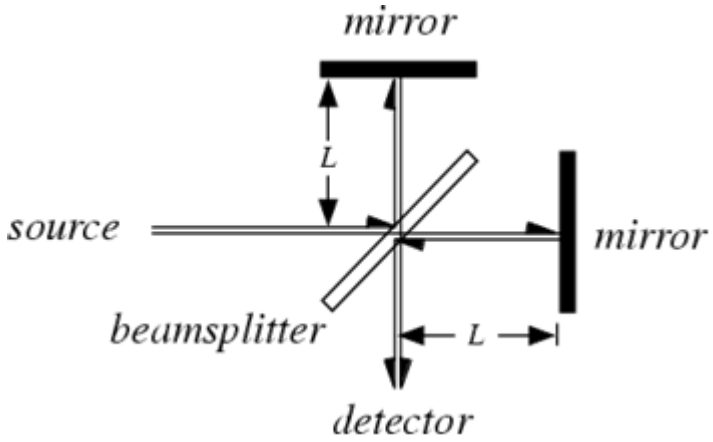

Figure 2.3: Schematic diagram of Michelson spectrometer.[28]

The radiation from the source is split into two beams by means of a beamsplitter (in the Michelson Morley experiment this was a half silvered mirror). One beam is reflected off a fixed mirror and one off a movable mirror, which establishes a time delay for one beam's arrival at the detector with respect to the other's. The interference of beams is only to measure the coherence

of the light at regular time delay setting. More specifically, the reflected light beam reaches the fixed mirror after traveling a distance *L*, which is called the *physical distance*, and returns to the beamsplitter after traveling a distance equal to 2**L*, which is called the *optical path*. Assuming that the two mirrors are at the same distance from the beamsplitter, the transmitted beam that reaches the movable mirror would have traveled the same optical path 2**L*. In fact, since the movable mirror travels back and forth around the distance *L* by an amount equal to δx, the transmitted beam returns to the beamsplitter after it has traveled a distance of $2(L + \delta x)$. Thus, the two beams recombine at the beamsplitter with an *optical path difference*, also called retardation, of $2*\delta x$.

The interference of the recombined beams could be either constructive or destructive, if the optical path difference and the wavelength of the light have the following relationship, respectively:

(1) Constructive interference $2*\delta x = n*\lambda$ $n = 1, 2, 3\ldots$ (8)

(2) Destructive interference $2*\delta x = (1/2)\ n*\lambda$ $n = 1, 3, 5\ldots$ (9)

Consequently, the intensity of the output beam would depend on the amount of constructive interference, which also depends on the optical path difference and on the wavelength of the incident radiation. For an optical path difference of zero, which is called the *zero path difference* (ZPD), all wavelengths of light would constructively interfere and a maximum intensity would be attained. The plot of detector response as a function of optical path difference is called an *interferogram*.

The shape of the *interferogram* significantly depends on the characteristics of the light source. For example, the *interferogram* of a monochromatic source, with only one wavelength,

would be a cosine function and the Fourier transform of this *interferogram* would give a single main peak in the final spectrum. On the other hand, for a broad lamp source that has a continuous infinity of wavelengths, the *interferogram* will be the sum of all the cosine waves that belong to each distinct wavelength present. In Fig. 4 are presented an ideal *interferogram* of a broadband source and a common *interferogram* obtained from experiments.

Besides optical accessories such as mirrors, beamsplitters, apertures, etc. that allow the interaction of infrared radiation with the sample and the collection of this light into a detector, a typical Fourier transform spectroscopic system also contains an analog optical transducer with input/output optics, which is the computing system that automatically performs the Fourier transformation of the *interferogram* into the desired spectrum, or a digital computer that performs this function. Thus, the infrared spectroscopic results can be obtained using a Fourier transform by measuring the signal at several discrete positions of a moving mirror. Even for bright sources, the IR interferometer has a very high spectral resolution.[27] The detected intensity as a function of moving mirror position, I(x), can be converted into the intensity spectrum as a function of frequency by the Fourier transform.

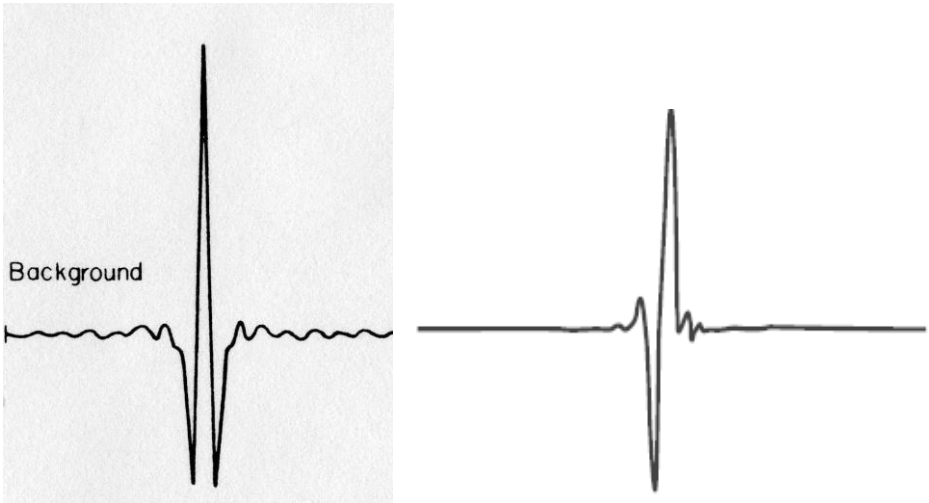

Figure 2.4: Ideal and experimental interferograms for a broadband source.[24]

In a typical IR transmission or absorption measurement, two steps should be performed. First, with no sample, a reference background should be taken, which is actually the response of the detector $I_0(\upsilon)$. Second, with the sample in place, another recording of $I_T(\upsilon)$ is taken. When the frequency of the incoming energy matches the frequency of the vibration of the molecules, part of the radiation is absorbed and part is transmitted, as shown graphically in Fig. 5.

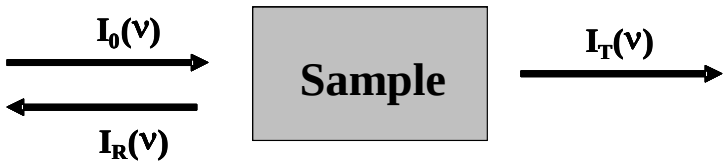

Figure 2.5: Schematic representation of incident, reflected, and transmitted light

The relation between the two light beam intensities $I_T(\upsilon)$ and $I_0(\upsilon)$, where the reflection from two sample surfaces (as is true in the case of pellets, which is the form of each of our samples) is neglected, is given by the well-known Bouguer-Lambert-Beer law of absorption of light by a partially transmitting medium:

$$I_T(\nu) = I_0(\nu)\, e^{-\alpha(\nu)\, d} \qquad (10)$$

where I_0 and I_T denote the intensities of the incident and transmitted beams at a specific wavenumber (ν), α is the linear absorption coefficient at a specific wavenumber, and d is the

thickness of the sample. The IR spectrum obtained is called the transmittance, and is the ratio of $\frac{I_T(\nu)}{I_0(\nu)}$, and is automatically calculated by the computer.

2.3.1 FT-IR experimental set-up.

The system used for infrared absorption analysis is a high-resolution vacuum based *Bruker IFS 66v*. This system and its schematic optical path are presented in Figs. 6 and 7, respectively. As can be depicted from Fig. 7 the *Bruker IFS 66v* system is essentially a Michelson type two-beam interferometer, with basic components such as the collimating optics, a fixed mirror, a beamsplitter and a movable mirror. In addition, to compensate for imperfections in the mirror movement, this system has a dynamical alignment control accessory.

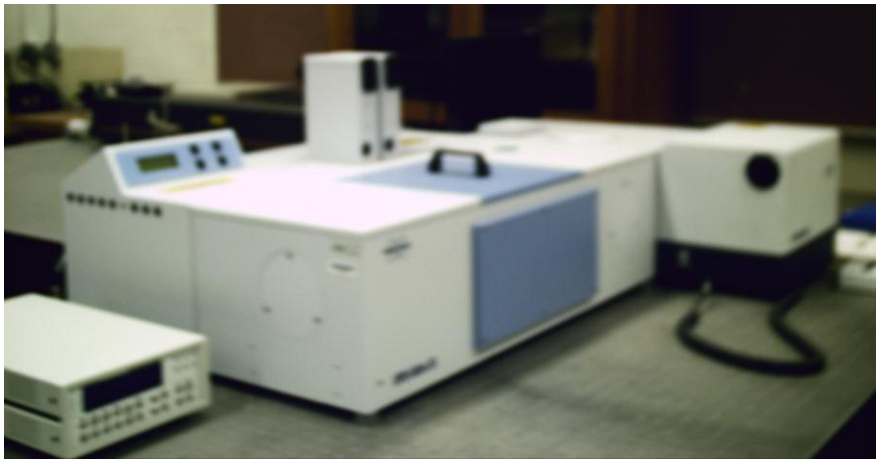

Figure 2.6*: Bruker IFS 66v* Fourier Transform Interferometer (FT-IR).[33]

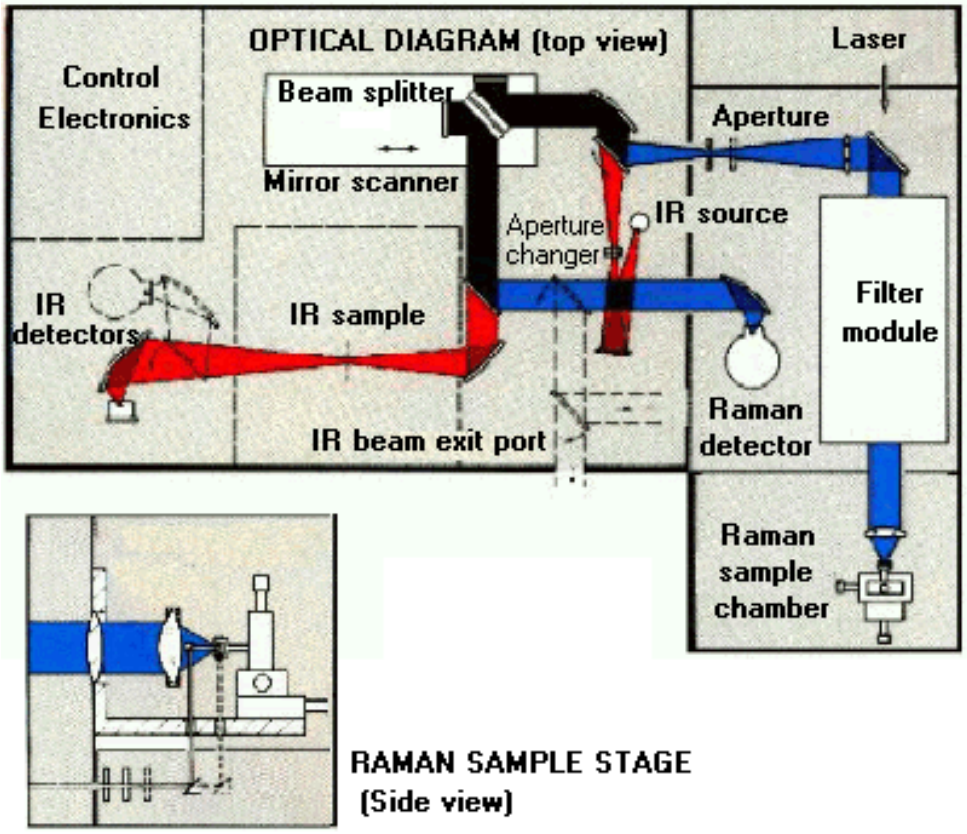

Figure 2.7: Schematic view of Bruker IFS 66v optical path.[33]

Also, as can be observed from Figs. 6 and 7, the parts of the instrument and their purposes are as follows:

- *The source*: the black body source emits predominantly infrared radiation. This radiation is passed through an aperture in order to control the amount of energy falling on the sample.
- *The interferometer:* the beam goes through the interferometer where the spectral encoding takes place. The resulting interferogram signal is produced by the interferometer.

- *The sample:* the modulated beam enters the sample compartment where it is transmitted through or absorbed by the sample. Depending on the type of analysis, various characteristics of the sample are observable.
- *The detector:* the beam finally passes to the detector for final measurement. Usually, semiconductor detectors are used for infrared detection.
- *The computer:* the measured signal is digitized and sent to the computer where the Fourier transformation takes place. The infrared spectrum is then presented to the user for any further manipulation.

Since a molecule exposed to an infrared beam during FT-IR analysis absorbs energy at frequencies characteristic of that molecule, for a typical specimen, plotting eitherthe absorption or the transmission of the infrared rays as function of frequency yields spectral information consisting of peaks or dips, respectively. The outcome of the FT-IR spectrum is then analyzed and matched with known signatures of already identified materials that have been collected in FT-IR libraries. To perform FT-IR analysis, small quantities of material, whether solid, liquid or gaseous, are required. When an FT-IR library does not provide an acceptable match, individual peaks in the FT-IR plot may still be used to yield some useful information about the specimen.

It is worth noting that any absorption/transmission spectrum can be obtained in three different regions of the infrared radiation, depending on the properties of the sample that need analyzing. The three regions are:

i) Near Infrared (NIR) from 12500 to 4000 cm^{-1},

ii) Mid Infrared (MIR) from 4000 to 400 cm^{-1}, and

iii) Far Infrared (FIR) from 400 to 5 cm^{-1}.

To measure in a specific infrared radiation region, a specific light source, detector, and beamsplitter have to be selected. In the present work a Globar lamp, which is a silicon carbide rod,[21] was the source. It operates in the range of 20 cm^{-1} – 10,000 cm^{-1}. The detector employed was a DLATGS (deuterated l-alanine-doped triglycine sulfate), which operates at room temperature in the 360 cm^{-1} to 12,000 cm^{-1} range. The beamsplitter we used was a KBr beamsplitter with a characteristic range of 370 cm^{-1} – 7500 cm^{-1}.

2.4 COMPARISON BETWEEN RAMAN AND INFRARED ABSORPTION SPECTROSCOPIES

Although both infrared absorption and Raman spectroscopies provide information about vibrational and rotational energy levels of molecules in materials, FT-IR is a direct absorption process whereas Raman is a scattering process; thus, these two techniques work on different selection rule principles and offer information regarding different symmetries of functional groups. For instance, symmetric diatomic molecules do not exhibit a change in the dipole moment; therefore, they have an indistinct infrared absorption spectrum. However, because stretching and contraction of the bonds change the interactions between electrons and nuclei, which in turn change the molecular polarizability, they do have a definite Raman spectrum. Even for highly symmetric polyatomic molecules which have a center of inversion, such as benzene, bands that are infrared active are not Raman active. Molecules with less symmetry are likely to be both infrared and Raman active. Carbonyl groups and nitriles always have strong IR signatures whereas aromatic rings and carbon double bonds lead to intense Raman bands.

In summary, we can state that asymmetric molecular structures that undergo changes in electric dipole moments during molecular vibration are IR active, while symmetric molecular structures that undergo changes in electron polarizability during vibration are Raman active.

Also, since infrared absorption occurs when a sample is irradiated by a stream of photons of different energies, the molecules usually absorb only certain characteristic energies that match their natural vibrational states. Thus, usually, the sources of light employed in infrared absorption measurements are infrared sources which correspond energetically to ranges of a few tens of MeV; this corresponds to the $10^4 – 10^2$ cm^{-1} frequency range or also to the infrared region of the electromagnetic spectrum. While the absorption frequency depends on the particular vibrational state, the amount of absorption depends on the effectiveness of the transfer of energy between the photon and the molecule, which in infrared spectroscopy is dictated by the change in the dipole moment occurring in the molecule as a result of the vibration.[21]

On the other hand, in Raman scattering, monochromatic sources of radiation such as lasers are used. When the electric field component of the light source interacts with a molecule it induces, as mentioned above, a dipole moment, which depends on the polarizability of the material under study. Energy range matching between source radiation and the characteristic vibrational states of different molecules is unnecessary in this scenario, and symmetric structures have dominant Raman signatures.

2.4.1 Advantages and disadvantages of infrared absorption and Raman spectroscopic techniques

Another aspect that is worth noting is the type of the sample that needs to be analyzed. For example, aqueous solutions give major difficulties in FT-IR measurements, but they can be easily characterized by Raman scattering. The reason behind this is the water strongly absorbs light at mid infrared wavelengths, but it is a weak Raman scatterer. So, Raman has great impact in the study of live microbiological samples, an application for which infrared absorption spectroscopy is not suited.

Also, when materials are exposed to visible light, there is a chance of observing fluorescence or photoluminescence. Visible and UV laser excitation sources induce these emissions, whereas infrared sources do not. Hence, FTIR spectroscopy does not show these emissions, but the Raman scattered light can be completely masked by them. In Raman spectroscopy, use of near infrared laser diodes often allows fluorescence problems to be avoided.[29] Combined use of both techniques has many benefits in achieving appropriate sensitivity for each of a variety of different functional groups.

Sample preparation is another aspect that needs consideration. Usually, the samples for infrared absorption measurements are prepared by embedding the material under study into a transparent matrix, namely a substance that is non-absorbing in the energy range of interest, and pressing the resulted compound into pellets. All the samples analyzed in this work were prepared as pellets with potassium bromide (KBr) as the matrix. KBr is transparent in the region of interest, and the only precaution that should be observed is to avoid any water contamination. Also, only a small amount of sample material needs to be ground together with KBr, and then pressed into a thin film with the help of a die and a hydraulic press.

The sample preparation for Raman scattering experiments is simpler. The sample to be analyzed just needs to be placed on any solid surface, such as a glass slide or in aqueous solution.

In summary, the particular strengths of FT-IR include the following:

- It is fast
- Enables collection of high quality data over a full energy range
- Prevents interference from fluorescence from organic impurities.

Raman, on the other hand:

- Allows analysis with less demanding sample preparation

- Permits measurements of liquid samples that use water as a solvent.

In conclusion, each technique has its own advantages; thus, by using them both, an extensive range of materials can be analyzed; materials with application in the scientific, forensic, pharmaceutical, biomedical, and semiconductor industries.

2.5 SAMPLE PREPARATION

The single diffusion gel growth technique has been amply explained in the literature since it is one of the most popular techniques for growing calcium oxalate crystals in laboratory.[30,31,32] It is also the sample preparation technique used in this work to grow the crystals without and with different concentrations of nordihydroguaiaretic acid (NDGA). Thus, the synthesis of the samples is very similar to the ones reported by many researchers. The chemicals used in sample synthesis were purchased from Sigma-Aldrich, whereas the Knox gelatin was purchased over the counter.

A detailed explanation of the gel growth technique employed here is as follows:

2.5.1 Preparation of stock solutions

Two 0.4M stock solutions, one of calcium chloride and one of potassium oxalate, were prepared by mixing 7.35g calcium chloride and 9.2g potassium oxalate, respectively, with 125ml distilled water under vigorous stirring in order to assure solution homogeneity. To the calcium chloride stock solution, 3.47g of potassium chloride at a 0.4mM was added again under continuous stirring. The reason behind the addition of potassium chloride was to prevent potential formation of hydrochloric acid, which could contribute to the dissolution of the resulting crystals.

2.5.2 Preparation of Knox gelatin solution

To the calcium chloride stock solution, 14.28g of Knox gelatin was added under vigorous stirring and moderate heat to form a melted gelatin solution. The pH of this gel solution was adjusted to 5.5 by titration with small volumes of concentrated HCl (10M), then equally divided into five different beakers, each containing 25 ml, which were left to cool until the gelatin congealed.

2.6 GENERAL ARRANGEMENT OF SAMPLES' ASSEMBLY

The general sample assembly is presented below in Figure 8 and is as follows: nordihydroguaiaretic acid solution, which is also called masoprocol, was prepared at different concentrations of 25µM, 50µM, 75µM and 100µM. When the Knox gels were perfectly set, different concentrations of masoprocol was poured gently into the respective beakers. One beaker was left without masoprocol. Next, 25ml of the 0.4M potassium oxalate stock solution was poured on each top layer of gel solution.

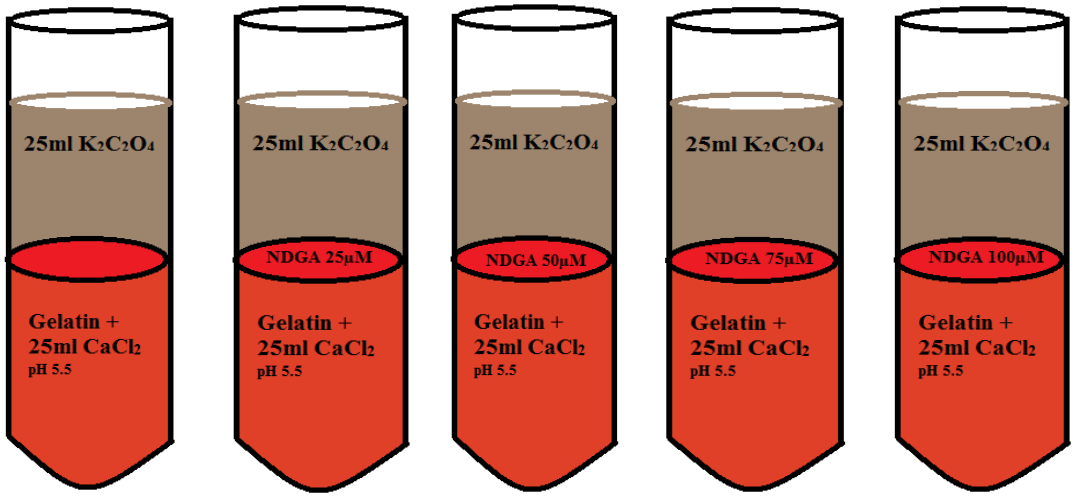

Figure 2.8: Schematic representation of beakers with gel solutions and different concentrations of NDGA

Then, the beakers were covered tightly with aluminum foil and the diffusion process was allowed to take place at the gel-liquid interface, which lead to the formation of crystals. After a few weeks the resulting crystals were harvested and analyzed.

Chapter 3: EXPERIMENTAL RESULTS AND DISCUSSIONS

3.1 INTRODUCTORY REMARKS

Recently, a scientific study was done by Manciu's research group[36,37] using infrared (IR) absorption and Raman spectroscopy on synthetically grown calcium oxalate calculi and their successive size decrease based on the use of herbal extract from Larrea Tridentata, which is a common shrub found in El Paso desert region. This plant belongs to the Zygophyllacea family and has the characteristic of remaining green in any season. It is bitter in taste and toxic.

In the laboratory, the previously described single diffusion gel method was used to grow the crystals. Researchers harvested the crystals, and observed their size and shape under the microscope. Also, Raman and Fourier transform spectroscopic measurements were carried out on samples at different spots.

With increasing amounts of Larrea Tridentata herbal infusion in the beakers, they found that calcium oxalate crystal size was decreased significantly, as presented in Figs. 1(a)-(d).[36,37] Moreover, the crystals' color changed from white transparent for pure crystals to light orange–brown for crystals grown with the inhibitor. Initially, the pure crystals have smooth surfaces; with the addition of herbal infusion the researchers found that the crystal shape changes, becoming irregular. This information was obtained when they analyzed the small crystallites under the microscope. Without infusion of herbal extract, crystals remained spherical, whereas with herbal inhibition, crystals take a tetragonal dipyramidal shape (see Fig. 1).

Not only that the researchers observed microscopic clear modifications into the appearances of the crystals, but, by spectroscopic analysis, they were able to distinguish crystals'

structural modifications arising in this complex process, such as their transformation from a monohydrate to a

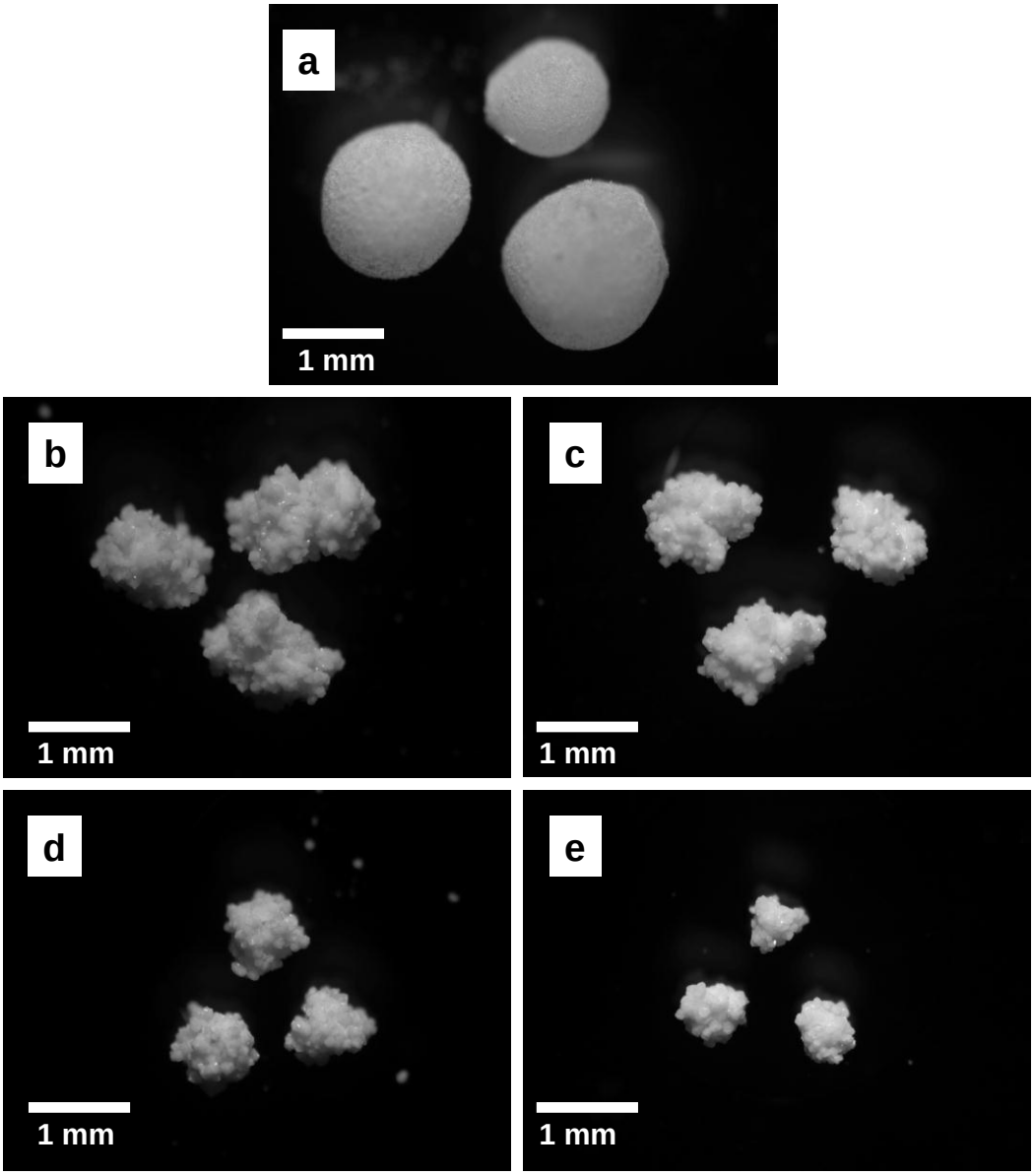

Figure 3.1: Calcium oxalate calculi grown: (a) without the herbal extract, and (b) – (d) with different concentrations of *Larrea Tridentata*. [36,37]

dehydrate structure. Commonly, in calculi, calcium oxalates appear in two forms: calcium oxalate monohydrate (COM) and calcium oxalate dihydrate (COD) (see Fig. 2). Compositionally, they are almost identical by having two carbon atoms and one calcium atom. The only difference is that COD is loosely bound with two water molecules, whereas COM is associated with only one water molecule.

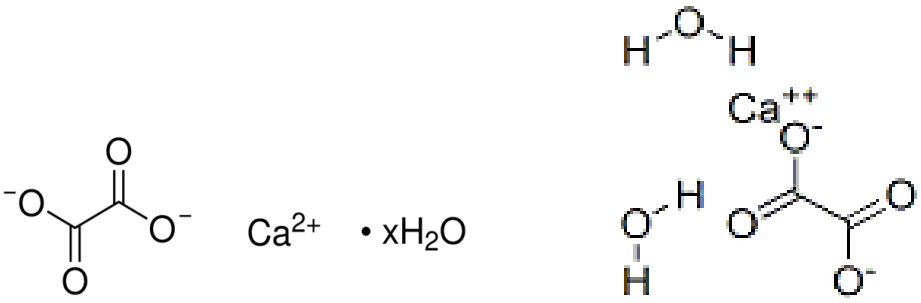

Figure 3.2: Molecular structure of COM and COD[38,39]

Raman spectroscopy is a convenient and suitable method for differentiating the two phases of calcium oxalates. A doublet or a single peak forms in the 1200 – 800 cm^{-1} region for COM and COD, respectively.[3,4] These are strong vibrations belonging to symmetrical carbonyl COO^- modes, and are characteristics of this phase transition. Thus, by employing Raman spectroscopy, the researchers found that under the influence of herbal infusion, transformation of samples from COM to COD took place. Figure 3 shows the comparison of the Raman data of the monohydrate structure (COM) of the crystals grown without the inhibitor, as well as the characteristic features like O-C-O bending vibrations and C-C stretching vibrations which are shifted to higher wave numbers in the spectra with the inhibitor. [36]

Other evidences of the structural modification of the crystals under the inhibition of *LarreaTridentata* extract were observed by the researchers on the IR spectra for the crystallites

(see Fig. 4), which showed characteristic absorption lines of COM in the higher wavenumber region at 3057, 3258, 3340, 3430, and 3492 cm^{-1}.[36,37] In the same spectroscopic frequency window, only a strong broad absorption band was observed in the Larrea Tridentata infusion spectrum. Furthermore, only a very strong and sharp absorption line was seen in IR spectra of the crystals grown with the inhibitor, band which does not resemble the characteristic absorption of COD structure. Thus, another inhibition mechanism might contribute as well with specific characteristic bonding between functional groups of the calcium oxalate crystals and the inhibitor.

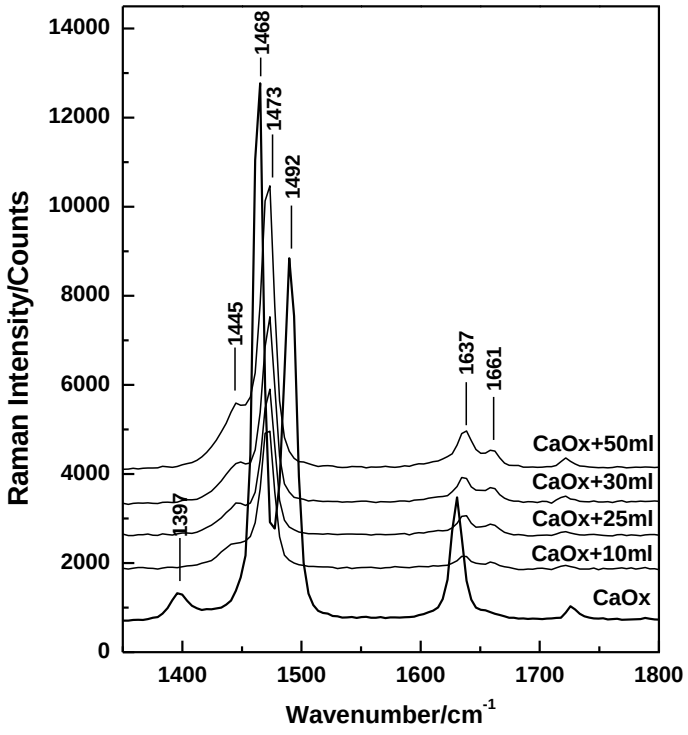

Figure 3.3: Raman spectra of calcium oxalate crystals without and with Larrea Tridentata inhibitor, as labeled, for the frequency range 1350 – 1800 cm^{-1}.[36,37]

Per authors finding, this inhibition mechanism was associated with the bonding between Mg^{2+} from Larrea Tridentata and oxalate ions from the calcium oxalate crystal surface. Also, per authors' suggestion, since literature studies indicate that NDGA is a dominant component in the Larrea Tridentata, another explanation of this strong absorption seen in the higher wavenumber region, is its association with NDGA or, more probable, with its chemical derivatives.

Finally, per authors discovery and as presented in Fig. 5, the crystal color was darker in the core, indicating dominance of organic material, and also unevenly covered by a thin shell of magnesium oxalate.[36,37] These magnesium oxalate shells served as passivation layer around the surfaces of the crystals. After some time, reduced size calcium oxalate crystals (kidney stones) start growing and form aggregates because some of the magnesium oxalate shells do not fully surround the crystals.

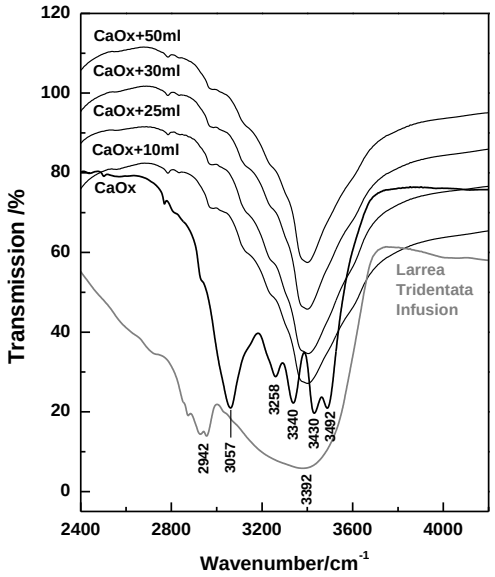

Figure 3.4: Infrared absorption spectra of crystals without and with Larrea Tridentata inhibitor and the spectrum of the Larrea tridentata infusion alone, as labeled, for the frequency range 2400 – 4200 cm^{-1}.[36,37]

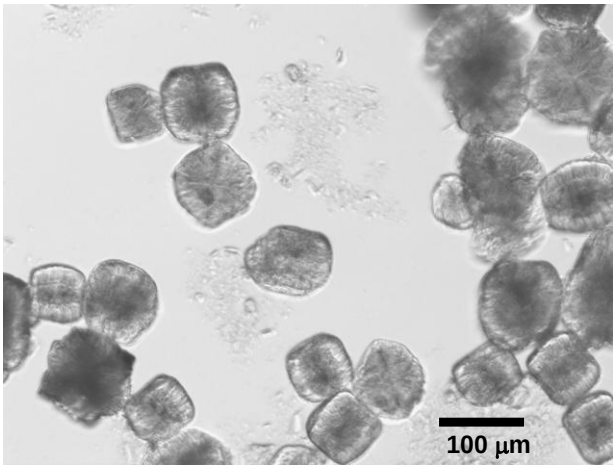

Figure 3.5: Micrograph of crystals grown with 30 ml Larrea Tridentata infusion, showing darker cores with outer layers of transparent thin shells.[36,37]

Solving this complex problem requires further study of calcium oxalate crystals. Since NGDA, a proven antioxidant, is the most important component of Larrea Tridentata, a logic continuation of this study is the use of NDGA as inhibitor in the growth of calcium oxalate crystals. Thus, the objective of this work is to check whether NDGA or other chemicals present in the herb are responsible for the decrease in the sizes of these crystals.

3.2 NORDIHYDROGUAIARETIC ACID (NDGA)

Nordihydroguaiaretic acid (NDGA) is a compound found in the long-lived creosote bush (Larrea Tridentata). The Larrea Tridentata leaves and stem has high quantities of the NDGA's phenolic compound, which has a crystalline solid form. A schematic chemical representation of NDGA is shown in Fig. 6.

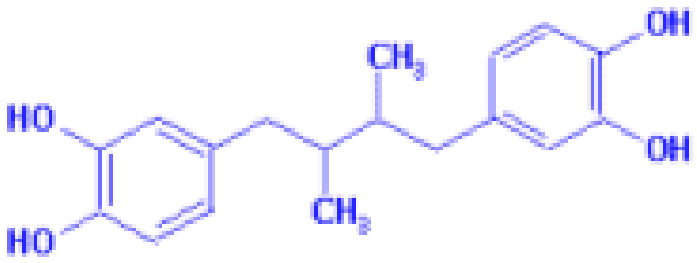

Figure 3.6: Chemical structure of NDGA[40]

NDGA could be responsible for the bush's long life, due to its capacity for reducing cell damage by free radicals. From research studies in 1986, female mosquito's average life span increased by 50 percent (from 29 days to 45 days) with NDGA injection. NDGA is also proven as a mouse life extension compound. The plant has been used to treat a variety of illnesses including infertility, rheumatism, arthritis, diabetes, gallbladder and kidney stones, pain and inflammation. During the 1950s, this plant was widely used as a food preservative for natural fibers, but was later banned after reports of its toxicity. On account of this toxic behavior, its use became controversial. Recently, it has been used as a nutritional supplement, however, renal and hepatotoxicities have been reported for excessive use of creosote bush and NDGA.[40]

NDGA is a potent antioxidant. In NDGA, hydroxyl groups play an important role in inhibiting the monooxygenase activity, and act as antimutagen / anticarcinogen. NDGA also demonstrates antimicrobial activity. Researchers reported its protective role against the genotoxic damage, too.[41] Furthermore, due to its properties as an anti-irritant and an anti-inflammator for human skin, since is preventing the oxidation of natural skin oils, was used as an anti-aging skincare. So, NDGA is considered as most beneficial key ingredient in Larrea Tridentata plant.

3.3 RAMAN RESULTS OF NDGA INHIBITION OF CALCIUM OXALATE CALCULI

The Raman results of calcium oxalate crystals grown without or with NDGA, as well as the Raman spectra of NDGA itself, which is shown for comparison reasons, are presented in Figs. 7 and 8. At a glance, the addition of NDGA didn't make a visible vibrational modification in the Raman spectra of the crystals grown with this compound, *e.g.* the spectra show all the vibrations observed in the Raman spectrum of the pure crystals (crystals grown without NDGA); thus, no visible evidence of the presence of NDGA.

Furthermore, all these spectra show the existence of a strong peak doublet in the frequency range of 1450 – 1500 cm^{-1}, doublet which resembles the characteristic Raman vibrations of COM type of crystals. A closer introspection at the Raman spectra in the frequency region of the mentioned peak doublet is presented in Figs. 9 and 10. It is worth noting that with increasing concentration of NDGA inhibitor, the intensity of the second peak at 1490 cm^{-1} is decreasing. So, although a very slight one, there is an effect of NDGA on the growth of calcium oxalate crystals.

A closer introspection at the Raman spectra in the frequency region of the mentioned peak doublet is presented in Figs. 9 and 10. It is worth noting that with increasing concentration of NDGA

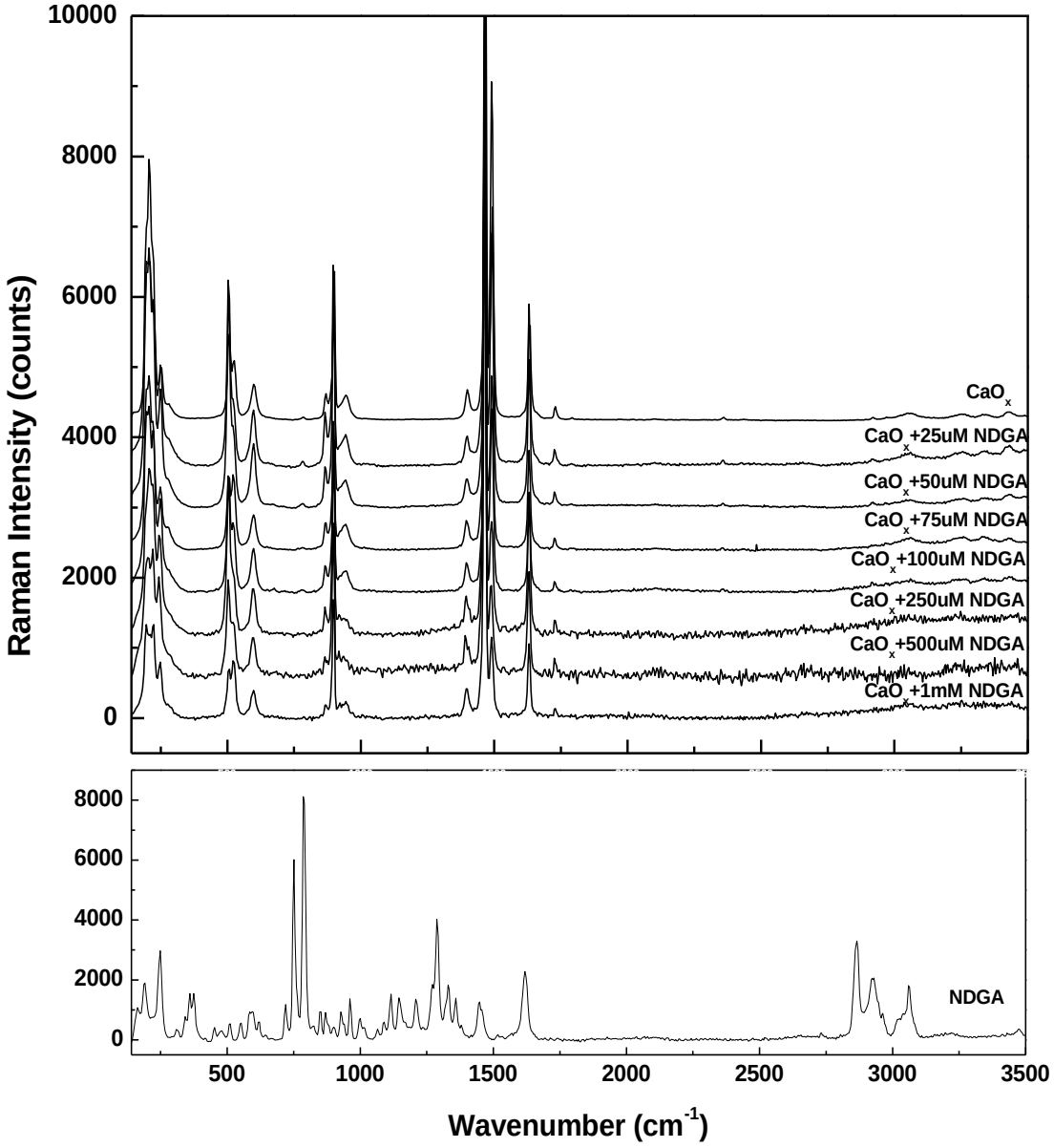

Figure 3.7: Raman spectra of crystals without and with 25 μM, 50 μM, 75 μM, 100μM, 250μM, 500μM and 1mM NDGA inhibitor and the spectrum of the NDGA alone, as labeled, for the frequency range 140 – 3500 cm^{-1}.

inhibitor, the intensity of the second peak at 1490 cm^{-1} is decreasing. So, although a very slight one, there is an effect of NDGA on the growth of calcium oxalate crystals.

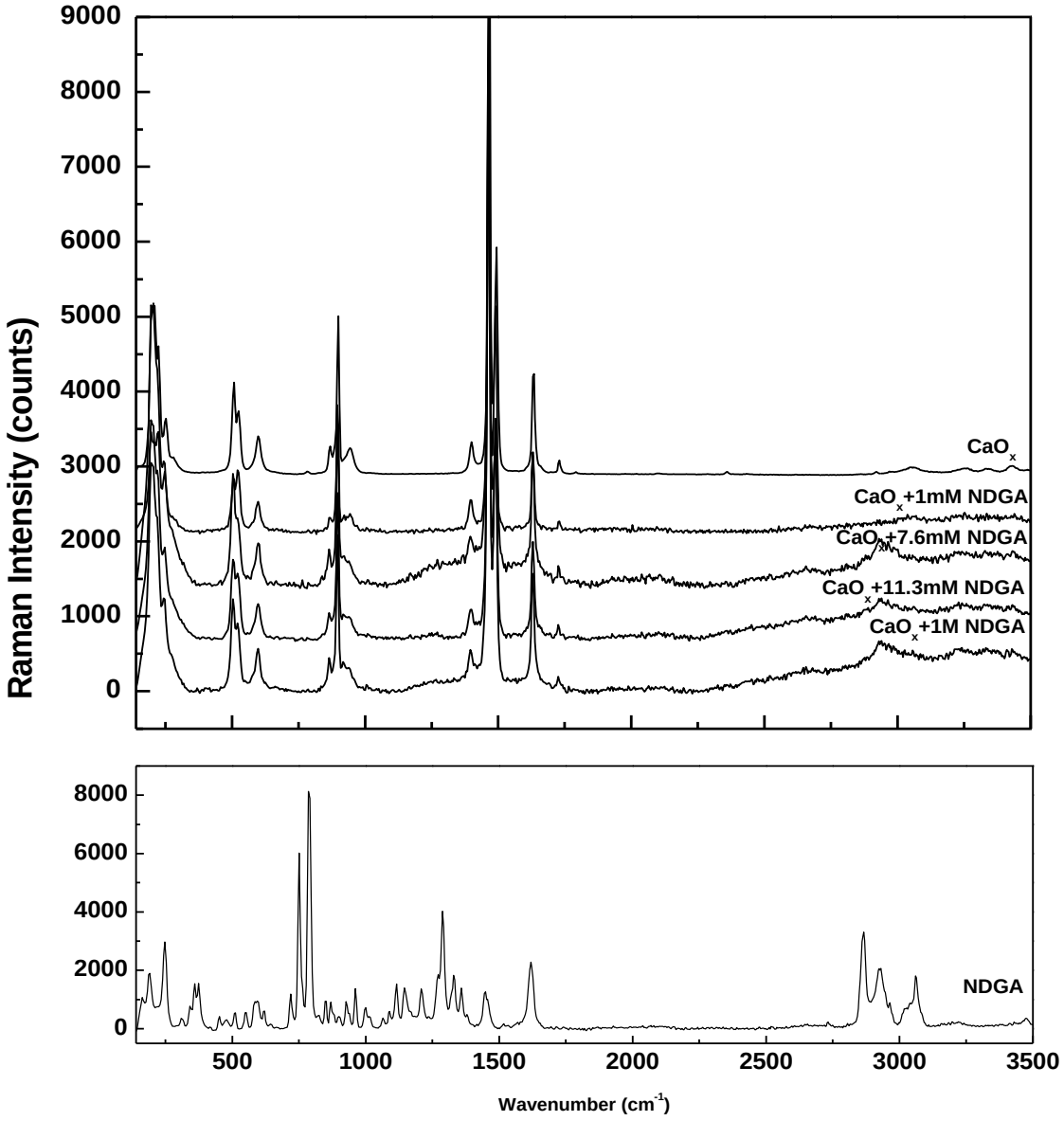

Figure 3.8: Raman spectra of crystals without and with 1M, 11.3mM, 7.6mM, and 1mM NDGA inhibitor and the spectrum of the NDGA alone, as labeled, for the frequency range 140 – 3500 cm^{-1}.

As stated above, these two vibrational lines that form this peak doublet are due to symmetrical carbonyl COO^- modes, and their intensities are associated with the lengths and strengths of C-C bonds of COM structure.[42,43] It is known that COM contains both planar and twisted oxalate units, with shorter C-C bonds in the twisted units than in the planar ones. Thus, as NDGA concentration increases, the difference in the C-C bonds lengths become larger, and, consequently, their strength too. More specifically, the C-C bonds in the twisted units become shorter in the crystals grown with NDGA than in those grown without the inhibitor.

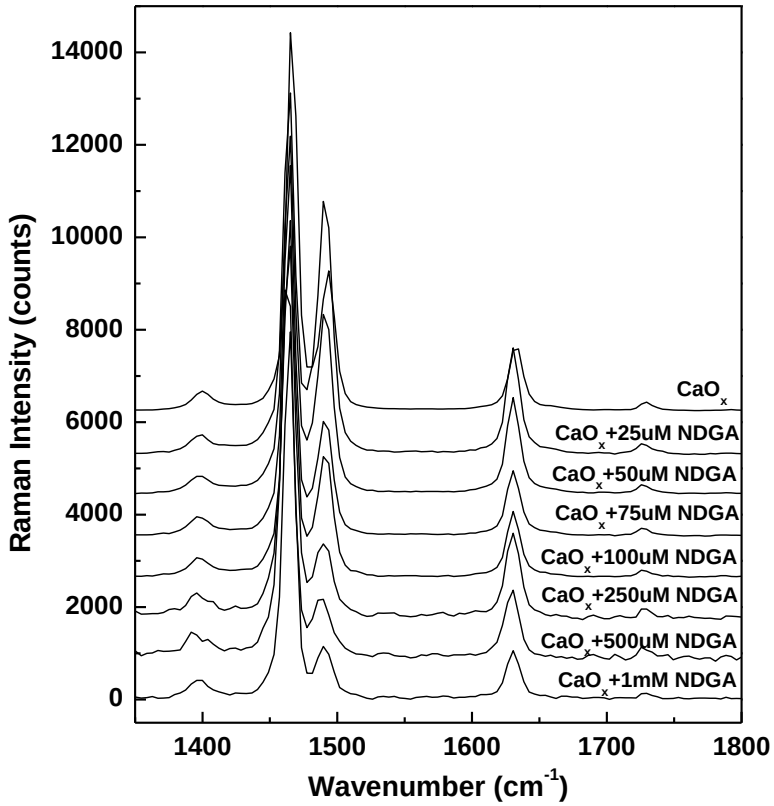

Figure 3.9: Raman spectra of crystals without and with 25 μM, 50 μM, 75 μM, 100μM, 250μM, 500μM and 1mM NDGA inhibitor, as labeled, for the frequency range1250 – 1800 cm^{-1}.

Also, from Fig. 9 can be observed that a "saturation" limit occurs with the increase of NDGA concentration, in the sense that no visible modification in the intensity of the peak at 1490 cm^{-1} is observed for a NGDA concentration > 1mM.

Figure 11 shows the Raman spectra of the crystals grown with and without NDGA in the low frequency region of 100 cm^{-1} to 1300 cm^{-1}. Again the presence of NDGA is not visible in these spectra; the observed vibrations are similar to those seen in the spectrum of the pure calcium oxalate crystals.

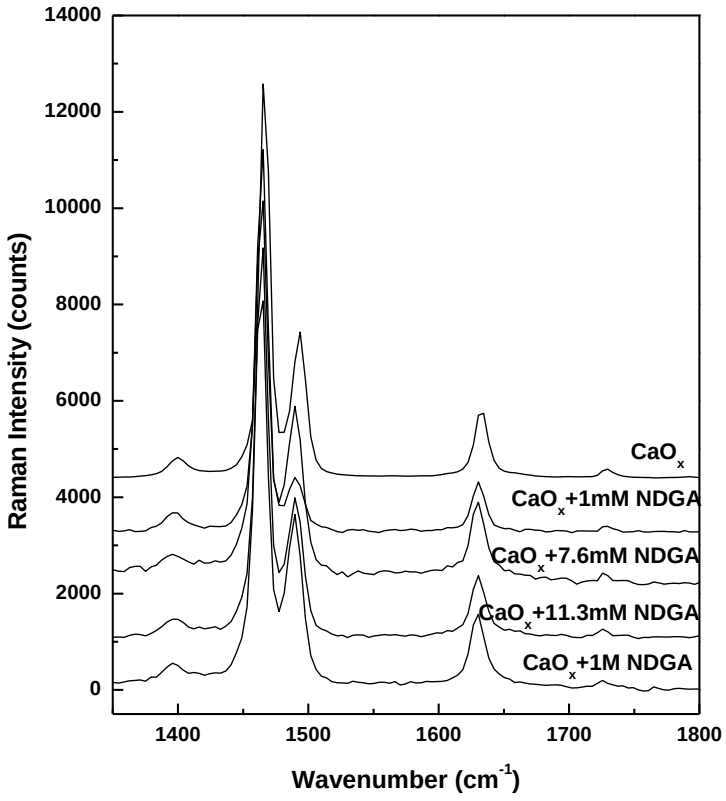

Figure 3.10: Raman spectra of crystals without and with 1M, 11.3mM, 7.6mM, and 1mM NDGA inhibitor, as labeled, for the frequency range 1300 – 1800 cm^{-1}.

Although the NDGA impact is very small, few vibrational changes could be observed in Fig. 11, too. For example, the broad band in the 200 cm^{-1} region, which contains a combination of three peaks, is decreasing in intensity with increasing NDGA concentration. Also, the peak doublet in the 500 cm^{-1} region of Fig. 11 demonstrates a behavior similar to that of the doublet in the 1400 – 1500 cm^{-1} region of Figs. 9 and 10. However, in the first case, at higher NDGA concentration, the intensity of the peak at 503 cm^{-1} is decreasing whereas the intensity of the peak at 526 cm^{-1} is increasing.

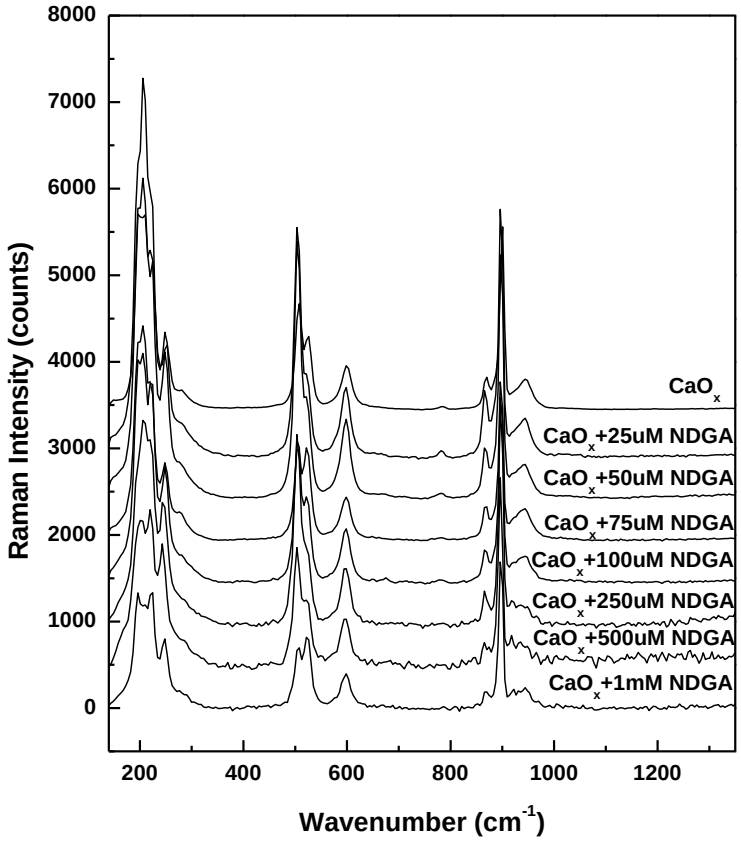

Figure 3.11: Raman spectra of crystals without and with 25 μM, 50 μM, 75 μM, 100μM, 250μM, 500μM and 1mM NDGA inhibitor, as labeled, for the frequency range 100 – 1300 cm^{-1}.

3.4 INFRARED ABSORPTION RESULTS OF NDGA INHIBITION OF CALCIUM OXALATE CALCULI

Other information about potential structural modifications of calcium oxalate crystals due to the influence of NDGA could be obtained from FTIR data. Therefore, next, we analyzed the samples using infrared absorption technique, and the results are presented in the following spectral regions: 1000 – 2500 cm^{-1}, 270 – 1200 cm^{-1}, and 2400 – 4000 cm^{-1}. For comparison purpose, we present the IR spectrum of pure NDGA, too.

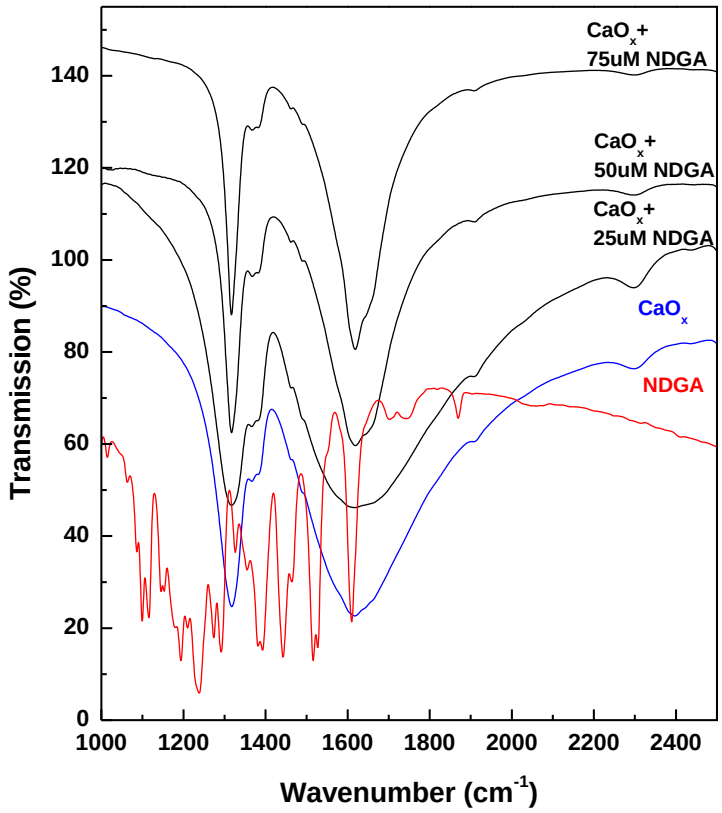

Figure 3.12: Infrared absorption spectra of crystals without and with 25 μM, 50 μM, and 75 μM NDGA inhibitor and the spectrum of the NDGA alone, as labeled, for the frequency range 1000 – 2500 cm^{-1}.

Since the existence of NDGA could be observed only in the spectral region of 1000 – 2500 cm^{-1}, we start our analysis with these IR results, which are presented in Figs. 12, 13, and 14. Although NDGA has numerous absorption lines in the frequency range of a 1000 – 1700 cm^{-1}, with increasing concentration of this compound, only a single vibrational line at 1610 cm^{-1} becomes visible; its intensity is increasing with NDGA concentration. There is no other influence that affects the morphology of the crystals grown with inhibitor, all the spectra resembling the one of the pure calcium oxalate crystals.

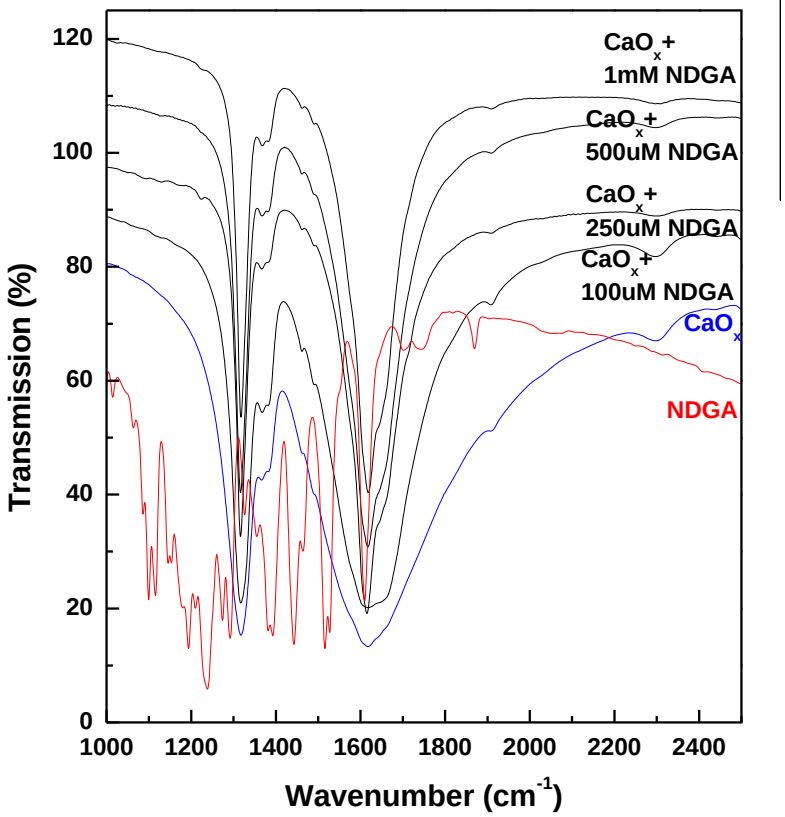

Figure 3.13: Infrared absorption spectra of crystals without and with 100 μM, 250 μM, 500 μM, and 1 mM NDGA inhibitor and the spectrum of the NDGA alone, as labeled, for the frequency range 1000 – 2500 cm^{-1}.

Furthermore, a direct confirmation of the fact that NDGA is the main ingredient of Larrea Tridentata plant and is chemically extracted from it, is, as observed in Fig. 15, the existence in both infrared spectra (the one of NDGA and the one of Larrea Tridentata) of the same 1610 cm^{-1} absorption line, which correspond to the C = C bonds of the ester group of NDGA.[44,45,46] Not only is this vibration common in both infrared spectra, but there is a similar overall absorption trend with similar absorption bands.

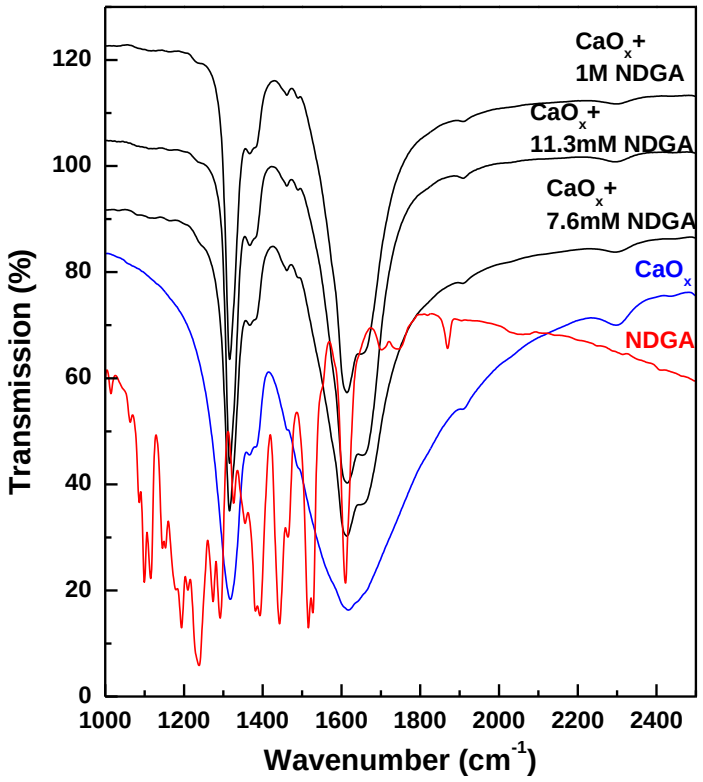

Figure 3.14: Infrared absorption spectra of crystals without and with 7.6 mM, 11.3 mM, and 1 M NDGA inhibitor and the spectrum of the NDGA alone, as labeled, for the frequency range 1000 – 2500 cm^{-1}.

The IR results for the crystals grown with different concentrations of NDGA, as labeled, for the other two spectral regions, namely the one of 270 – 1200 cm^{-1}, and the one of 2400 – 4000 cm^{-1}, are presented in Figs. 16, 18, and 20, and Figs. 17, 19, and 21, respectively. Even though in these frequency ranges the NDGA spectrum has absorption lines as intense as the 1610 cm^{-1} line, there is no evidence of the compound in these spectra.

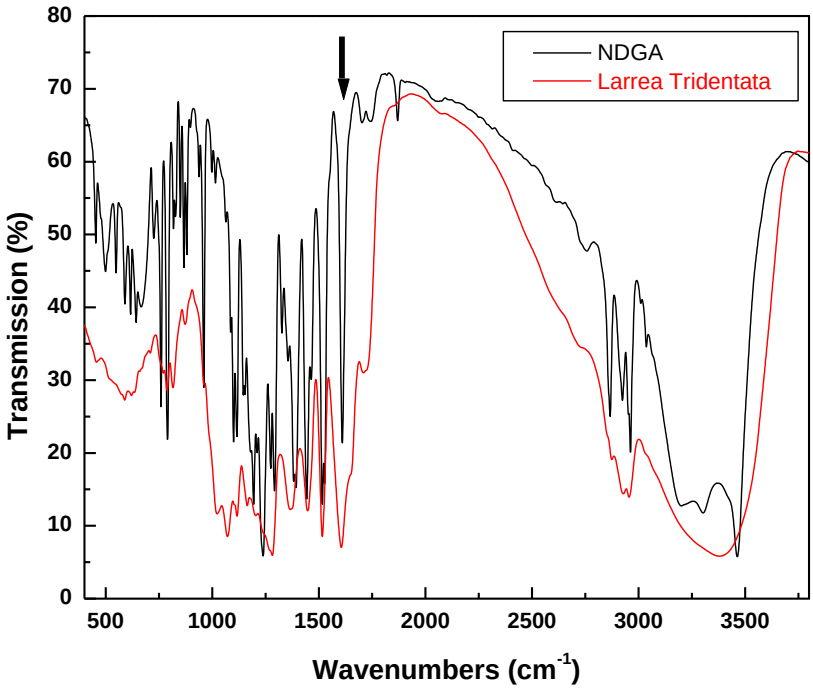

Figure 3.15: Infrared absorption spectra of NDGA and Larrea Tridentata.

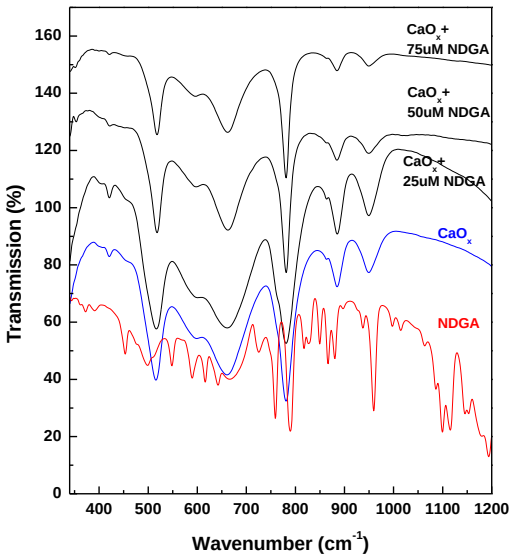

Figure 3.16: Infrared absorption spectra of crystals without and with 25 μM, 50 μM, and 75 μM NDGA inhibitor and the spectrum of the NDGA alone, as labeled, for the frequency range 340 – 1200 cm^{-1}.

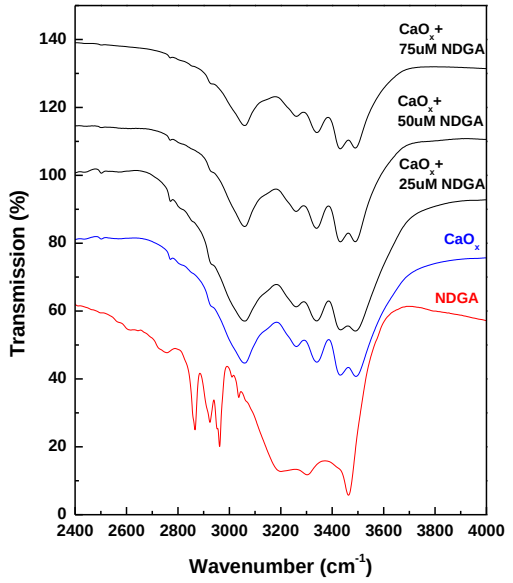

Figure 3.17: Infrared absorption spectra of crystals without and with 25 μM, 50 μM, and 75 μM NDGA inhibitor and the spectrum of the NDGA alone, as labeled, for the frequency range 2400 – 4000 cm^{-1}.

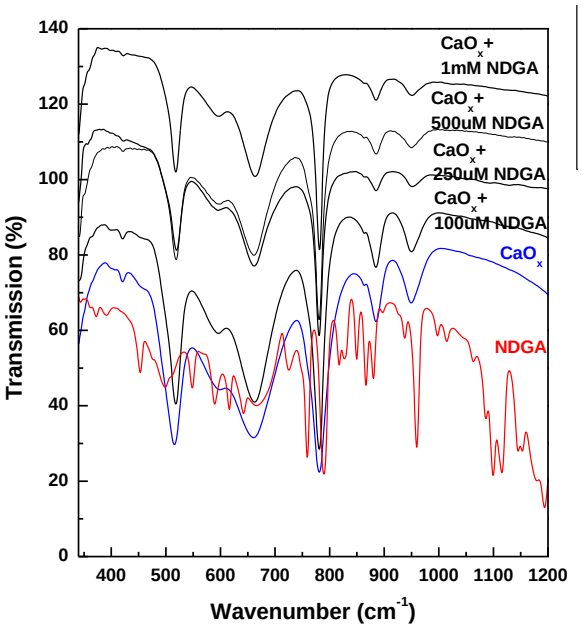

Figure 3.18: Infrared absorption spectra of crystals without and with 100 μM, 250 μM, 500 μM, and 1 mM NDGA inhibitor and the spectrum of the NDGA alone, as labeled, for the frequency range 340 – 1200 cm^{-1}.

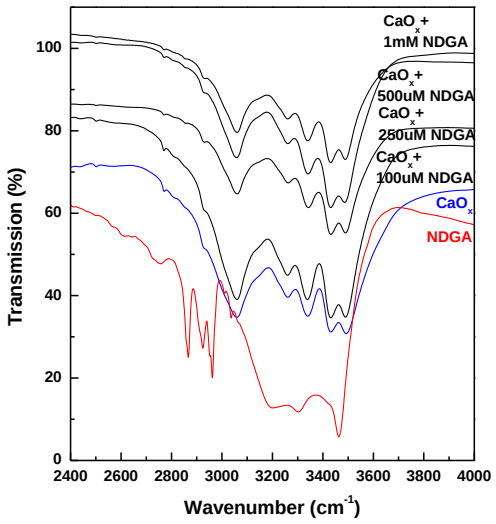

Figure 3.19: Infrared absorption spectra of crystals without and with 100 μM, 250 μM, 500 μM, and 1 mM NDGA inhibitor and the spectrum of the NDGA alone, as labeled, for the frequency range 2400 – 4000 cm^{-1}.

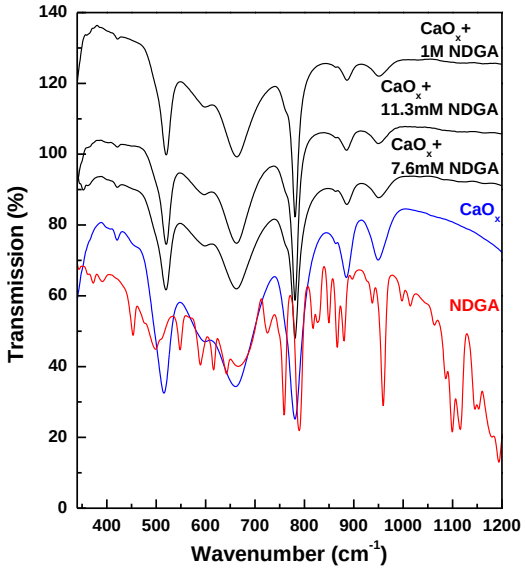

Figure 3.20: Infrared absorption spectra of crystals without and with 7.6 mM, 11.3 mM, and 1 M NDGA inhibitor and the spectrum of the NDGA alone, as labeled, for the frequency range 340 – 1200 cm^{-1}.

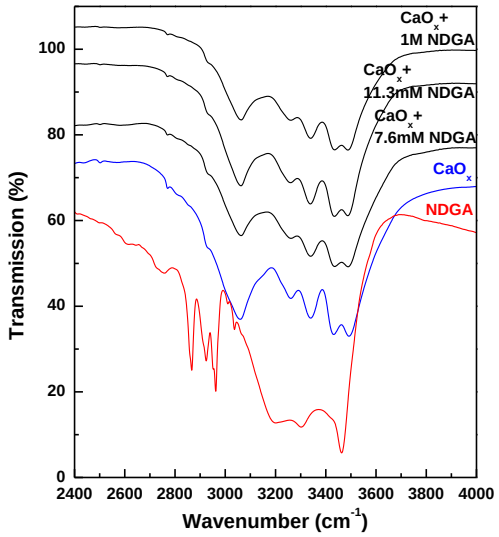

Figure 3.21: Infrared absorption spectra of crystals without and with 7.6 mM, 11.3 mM, and 1 M NDGA inhibitor and the spectrum of the NDGA alone, as labeled, for the frequency range 2400 – 4000 cm^{-1}.

Chapter 4: Conclusion

4.1 CONCLUSION

Urolithiasis is the process to form stones in kidney, bladder, and urethra. Stones form when urine contain too much of substances like calcium combine with oxalate, phosphate, or carbonate. A major risk factor to form kidney stones is dehydration. Kidney stones are of different types; they are calcium stones, cysteine, struvite, and uric acid stones. To treat kidney stones, the most general procedure is excess intake of fluids. Though any fluid can be taken, water is the ideal fluid for passing out small stones in the ureter. To treat larger stones many surgical methods are available such as extracorporeal shock-wave lithotripsy (ESWL), percutaneous nephrolithotomy (PNL), laparoscopic surgery, oral chemolysis, and open surgery. However, these methods are expensive and also they might present side effects. On the other hand, since traditional herbal medicine is more affordable, common people practiced it more.

In kidney stones' treatment, herbal medicine plays an important role in breaking the stones and also in preventing their further formation. Hydrangea, Chanca piedra, Chaparral (Larrea Tridentata), Scoparia dulcis, Punarnava, Varuna, Tribulus, Shigru, Apamarg, and Horsetail are plants used the most, since they are the best herbal remedies for kidney stones. However, for an efficient treatment using traditional medicine, knowledge of the chemical composition and structure of the stones is necessary. Since advanced techniques such as Raman and infrared absorption spectroscopies are employed in finding the chemical structures and compositions of different substances, these techniques are helpful in providing accurate analysis of the various urinary salts, from qualitative and quantitative aspects. For example, five different types of stones were found by spectroscopic analysis; they were calcium oxalate monohydrate

(COM), dicalcium phosphates dehydrate (DCPD), calcium phosphate hydroxide (CPH), calcium oxalate dihydrate (COD), and uric acid. Apart from Raman and FTIR, urolithiasis studies were done using optical microscopy and scanning electron microscopy (SEM).

Recently, F.S. Manciu's research group studied the inhibition of kidney stones using these spectroscopic techniques. They grew calcium oxalate crystals without and with the addition of Larrea Tridentata herbal extract using a single diffusion gel method, which is the same synthesis approach used in the current work. The researchers found that the harvested crystals had smaller sizes with increased amounts of Larrea Tridentata inhibitor. Also their shapes changed from spherical with smooth surfaces for pure crystals grown with no inhibitor addition to irregular agglomerates for crystals grown with Larrea Tridentata herbal extract. Furthermore, their color changed from white transparent for pure crystals to light orange – brown for crystals grown with the inhibitor.

Their further investigations of these samples by Raman and infrared absorption spectroscopies revealed a transformation from a calcium oxalate monohydrate (COM) structure for pure crystals to a dihydrate morphology for crystals with inhibitor. The researcher's suppositions regarding the causes that might contribute to the inhibition process were: a potential bonding between the Mg^{2+} from the plant with the oxalate ions from the crystal surface or the existence of an organic compound into this plant with inhibitory effects. Also, since an important ingredient of this plant is the nordihydroguaiaretic acid (NDGA), which is chemical extract from the plant, the current research is a logic continuation where we try to confirm whether or not NDGA is responsible for the inhibition process.

Thus, we synthetically grow in laboratory (following the same procedure of sol gel preparation method) calcium oxalate crystals with and without NDGA as inhibitor. Different

concentration of NDGA such as 25 µM, 50 µM, 75 µM, 100µM, 11.6 mM, 7.3 mM, and 1mM crystals were used in the actual synthesis. The harvested crystals were again investigated using Raman and infrared spectroscopies.

The results obtain from both spectroscopic techniques demonstrate that no structural transformation from COM to COD is taking place by using NDGA as inhibitor. However, although not dramatic, there is a contribution originating from NDGA in the current Raman data, namely a change in the intensity of the 1490 cm^{-1} vibration, which is one of the peaks that form the doublet characteristic to COM morphology. Since this vibration is associated with the length and strength of the C-C bonds in the twisted oxalate units and since is decreasing with increasing NDGA concentration, we assume that these bonds get shorter in the crystals grown with inhibitor.

Furthermore, the infrared data also demonstrate the existence of NDGA from the presence of an absorption line at 1610cm^{-1}, which get stronger with the increase in the compound concentration. This vibration correspond to C= C bond of the ester group of NDGA.

In conclusion, although present, NDGA is not responsible for crystals change in morphology; all the crystals have a COM structure without or with this inhibitor. Then, NDGA is not the dominant compound that contributes to the inhibition process.

REFERENCES:

1)http://emedicine.medscape.com/article/983884-overview

2)http://www.uptodate.com/contents/patient-information-kidney-stones-in-children

3)http://www.ncbi.nlm.nih.gov/pubmed/8936716

4)Soucie JM, Thun MJ, Coates RJ, McClellan W,Demographic and geographic variability of kidney stones in the United States.Kidney Int 1994; 46: 893-899.

5)http://www.ngc.gov/content.aspx?id=12528

6)http://www.modernmedicine.com/modernmedicine/Family+Medicine/Physicians-Focus-Radiation-Risk-in-Urolithiasis/ArticleStandard/Article/detail/671730

7)http://en.wikipedia.org/wiki/Traditional_medicine.

8)http://www.herbalcureindia.com/products/kidney-support.htm

9)http://www.jaherbs.com/index.php?option=com_content&view=article&id=59:carry-mi-seed&catid=25:the-herbs&Itemid=55

10)http://www.livestrong.com/article/166342-kidney-stone-surgery-side-effects/

11)Blijenberg BG, Baadenhuijisen H. Results of various analysis techniques in realation to urinary calculi studies. Brit J Urol 1987; 59: 159-163.

12)M daudon, C. Hennequin. Sex and age related composition of 10 617 calculi analyzed by infrared spectroscopy. Urological research 1995; 23: 319-326.

13)Ayoub kamoun, Michel daudon. Urolithiasis in Tunisian children: astudy of 120 cases based on stone composition. Pediatr Nephrol (1999); 13: 920–925.

14)Yi-Chun Chiu, Hao-Yu Yang. Detecting composition of urolithiasis by Raman spectroscopy after minimal invasive urological management. Proc. SPIE 2009.

15)Jing Z, GuoZeng W. Analysis of urinary calculi composition by infrared spectroscopy: a prospective study of 625 patients in eastern China.Urol Res, 2010; 38(2): 111-115.

16)Y.M Fazil Marickar, P.R Lekshmi Optical microscopy versus scanning electron microscopy in urolithiasis.Urological research, 2008; 37: 293-297.

17)S. Bisaillon, R. Tawashi Growth of calcium oxalate in gel systems. Journal of Pharmaceutical Sciences, 2006; 64: 458-460.

18)E. V. Petrova, N. V. Gvozdev Growth and Dissolution of calcium oxalate monohydrate (COM) crystals. Journal of Optoelectronics and Advanced Materials 2004;6:261-268.

19)http://en.wikipedia.org/wiki/Raman_spectroscopy#cite_note-Gardiner-0

20)http://content.piacton.com/Uploads/Princeton/Documents/Library/UpdatedLibraryRaman_Spectroscopy_Basics.pdf

21)N. B. Colthup, L. H. Daly, and S. E. Wiberley, Introduction to Infrared and Raman Spectroscopy, 3rd ed., Academic Press Inc., San Diego, 1990.

22)http://www.google.com/imgresimgurl=http://www.kosi.com/Raman_Spectroscopy/images/tutorial4.gif&imgrefurl=http://www.kosi.com/Raman_Spectroscopy

23)http://en.wikipedia.org/wiki/Fourier_transform_infrared_spectroscopy

24) http://mmrc.caltech.edu/FTIR/FTIRintro.pdf

25) http://www.wcaslab.com/tech/tbftir.htm

26) http://www.prenhall.com/settle/chapters/ch15.pdf

27) http://physics.schooltool.nl/irspectroscopy/method.php

28) http://scienceworld.wolfram.com/physics/MichelsonInterferometer.html

29) The combined inVia Raman and Illuminat*IR*. FT-IR spectrometer, SPD/AD/101 Issue 1.0, 2004.

30) D Valarmathi, Leela Abraham, S Gunasekaran, Growth of calcium oxalate monohydrate crystal by gel method and its spectroscopic analyzed, Indian Journal of Pure & Applied physics, 2009; 48: 36-38

31) N.V. Gvozdev, E.V. Petrova, T.G. Chernevich, Atomic force microscopy of growth and dissolution of calcium oxalate monohydrate (COM) crystals. Journal of Crystal Growth, 2004; 261: 539 -548.

32) M.J.Joshi, C.K. Chauhan, Growth inhibition of struvite crystals in the presence of herbal extract. Journal of Material Science, 2009; 20: 85-92.

33) http://midir.lightsource.ca/Manuals/Manual_IFS66vS.pdf

34) http://www.witec.de/en/products/raman/alpha300r/

35) V.S. Joshi, B.B. Parekh Herbal extracts of Tribulus terrestris and Bergenia ligulata inhibit growth of calcium oxalate monohydrate crystals in vitro. Journal of Crystal Growth 2005; 275: e1403-e1408.

36) L.A. Pinales, R.R. Chianelli, W.G. Durrer, R. Pal, M. Narayan, and F. S. Manciu, Spectroscopic study of inhibition of calcium oxalate calculi growth by Larrea Tridentata. Journal of Raman Spectroscopy, 2011; 42(3): 259-264.

37) Luis Alonso Pinales Ph.D thesis: "*Spectroscopic study of the inhibition of calcium oxalate calculi by Larrea Tridentata*"

38) http://www.chemicalbook.com/ChemicalProductProperty_EN_CB7154359.htm

39) http://www.chemspider.com/Chemical-Structure.108953.html

40) http://en.wikipedia.org/wiki/Nordihydroguaiaretic_acid

41) Yasir Hasan Siddique, Tanveer Beg, Protective effect of nordihydroguaiaretic acid (NDGA) against norgestrel induced genotoxic damage. Toxicology in Vitro, 2006; 20: 227-233.

42) P. Carmora, J. Bellanato, E. Escobar, Infrared and Raman spectroscopy of urinary calculi. Biospectroscopy, 1997; 3: 331-346.

43) V. R. Kodati, A. T. Tu, J. L. Turumin, Analysis of urinary calculi of mixed and unusual composition: Raman spectroscopic investigation Appl. Spectrosc, 1993; 47: 334-337.

44) Clark W. Perry Malda V, Kalnins Synthesis of Lignans. I. Nordihydroguaritic Acid. The journal of organic chemistry, 1972; 37(26): 4371-4376.

45) Hector Belmares, Arnoldo Barrera, New Rubber Antioxidants and Fungicides derived from Larrea Tridentata. Industrial & engineering chemistry product research and development, 1979; 18(3):220-226.

46) Jith Ru Hwu, Wen Nan Tseng, Antiviral Activities of Methylated Nordihydroguairetic Acids. 1. Synthesis Structure Identification, and Inhibition of Tat-Regulated HIV Transactivation. Journal of medical chemistry,1998;41(16):2994-3000.

CURRICULUM VITA

Preethi Dacha was born in Hyderabad, India. The first daughter of Shanker Dacha and Shashikala Dacha, she graduated from Pragathi High School, Wanaparthy, Andhra Pradesh, India, in the spring of 2001 and entered bachelors program at Osmania University College for Women's, Hyderabad, India. While pursuing bachelor's degree, she got Merit Certificate from National Graduate Physics Association (NGPA) for being placed in statewide top 1%, 2006. After her bachelor's, she worked as high school teacher for one year in Brilliant Grammar School, Hyderabad, India. In 2007, she joined in Master's program at VIT University, Vellore, India. There she got Merit scholarship award in 2009. Later, she worked on "Characterization of a Thomson X-ray Polarimeter and an X-ray crystal monochromator" under supervision of Dr. Biswajit Paul, Raman Research Institute (RRI), India. In the spring 2010, she joined into graduate school for Master's at University of Texas at Elpaso. In UTEP, she was awarded with Outstanding Graduate Teaching Assistant in April 2011.

Permanent Address: 15-48 Shanker gunj, Wanaparthy,
Mahaboobnagar, AP, India. 509103.
pdacha@miners.utep.edu.